and initiates apoptosis signaling by binding to and antagonizing the function of pro-survival Bcl-2 family members (Chen *et al.*, 2005). Our results indicate that lapatinib induces upregulation of BIM expression in *HER2* amplification-positive cells, and that depletion of BIM by RNAi results in marked inhibition of lapatinib-induced apoptosis in these cells. These data suggest that upregulation of BIM expression contributes to the induction of apoptosis by lapatinib in breast cancer cells with *HER2* amplification. We found that BIM induction by lapatinib occurred in *HER2* amplification-positive cells regardless of *PIK3CA* mutational status and was associated with inhibition of ERK phosphorylation. With the use of specific inhibitors of MEK, we also found that regulation of BIM expression is mediated by the MEK-ERK signaling pathway. These findings are consistent with those of previous studies showing that MEK inhibitors induce BIM expression in B-RAF mutant cells (Cragg *et al.*, 2008), and that inhibition of the MEK-ERK pathway contributes to BIM induction by EGFR tyrosine kinase inhibitors in non-small cell lung cancer (Costa *et al.*, 2007; Cragg *et al.*, 2007; Gong *et al.*, 2007), and that such upregulation of BIM has an essential role in the induction of apoptosis by these agents. We also found that ABT737 enhanced the induction of apoptosis by lapatinib in cells with *HER2* amplification regardless of *PIK3CA* mutational status, further supporting a role for BIM induction in lapatinib-induced apoptosis. To our knowledge, the present study is the first to show that induction of BIM through inhibition of the MEK-ERK pathway is required for lapatinib-induced apoptosis in breast cancer with *HER2* amplification.

Although lapatinib-induced upregulation of BIM expression occurred in a manner independent of *PIK3CA* mutational status, the pro-apoptotic effect of lapatinib was less pronounced in cells with an activating *PIK3CA* mutation than in those without one. Given that such *PIK3CA* mutations result in hyperactivation of the PI3K signaling pathway (Isakoff *et al.*, 2005; Zhao *et al.*, 2005; Berns *et al.*, 2007), we examined whether activation of this pathway was associated with this difference in the extent of apoptosis. Indeed, we found that lapatinib did not inhibit the phosphorylation of AKT in *HER2* amplification-positive cells with an activating *PIK3CA* mutation. We therefore examined the effect of specific inhibitors of the PI3K pathway on lapatinib-induced apoptosis in cells with a *PIK3CA* mutation. Treatment with BEZ235 effectively inhibited AKT phosphorylation, and the combination of BEZ235 and lapatinib thus inhibited both AKT and ERK phosphorylation and had a pro-apoptotic effect that was markedly greater than that observed with either agent alone. Consistent with these *in vitro* experiments, the combination of lapatinib and BEZ235 exhibits an enhanced anti-tumor effect *in vivo* with HER2-positive xenografts with a *PIK3CA* mutation. These results suggest that additional inhibition of the PI3K pathway is required for effective induction of apoptosis by lapatinib in cells with a *PIK3CA* mutation. Lapatinib shows clinical efficacy both alone and in combination with chemotherapeutic agents, but not all patients with *HER2* amplification-positive tumors respond to such treatment (Slamon *et al.*, 1987; Slamon, 1990; Geyer *et al.*, 2006; Di Leo *et al.*, 2008; Gomez *et al.*, 2008). *PIK3CA* mutations have been detected in 20–30% of breast cancer patients with *HER2* amplification (Saal *et al.*, 2005; Stemke-Hale *et al.*, 2008), and our data now suggest that activation of the PI3K signaling pathway associated with the presence of a *PIK3CA* mutation may be responsible, at least in part, for the limited efficacy of lapatinib in patients with tumors positive for both *HER2* amplification and a *PIK3CA* mutation. Similar to the effects of lapatinib, the MEK inhibitor AZD6244 inhibited ERK phosphorylation and increased BIM expression, without affecting AKT phosphorylation or survivin expression, and it cooperated with BEZ235 to induce apoptosis in *HER2* amplification-positive cells with a *PIK3CA* mutation (Supplementary Figure 3). These data thus indicate the importance of simultaneous interruption of the PI3K-survivin and MEK-ERK-BIM pathways for effective induction of apoptosis in such cells. However, the extent of apoptosis induced by AZD6244 alone or in combination with BEZ235 was less pronounced than that induced by lapatinib, suggesting that the anti-tumor effect of lapatinib in these cells is not mediated exclusively through inhibition of MEK-ERK signaling. Further investigation is thus needed to clarify the relationship of *PIK3CA* mutational status to the efficacy of lapatinib. The development of PI3K inhibitors has advanced substantially in recent years, and clinical trials of these agents alone or in combination with other anti-tumor agents are under way. Our study therefore provides a rationale for clinical evaluation of combination therapy with lapatinib and a PI3K inhibitor in breast cancer patients with *HER2* amplification and a *PIK3CA* mutation.

Survivin is essential for proper completion of various stages of cell division, with this protein having been found to contribute to centrosomal function, spindle formation and kinetochore attachment to spindle microtubules (Speliotes *et al.*, 2000; Uren *et al.*, 2000). Survivin is preferentially expressed during the mitotic phase of the cell cycle and is physically associated with the mitotic apparatus. It has also been found to be overexpressed in some tumors, with such overexpression having been associated with a poor clinical outcome (Ambrosini *et al.*, 1997; Tanaka *et al.*, 2000; Altieri, 2003). Like other members of the IAP family such as XIAP and c-IAP1, survivin contains a single BIR (baculoviral IAP repeats) domain. Molecular antagonists of survivin, including anti-sense and siRNA oligonucleotides as well as dominant negative mutants, have been shown to induce apoptosis (Olie *et al.*, 2000; Kanwar *et al.*, 2001), suggestive of an association between survivin and apoptosis. Consistent with these previous findings, we have now shown that depletion of survivin by two independent siRNAs specific for survivin mRNA increased the number of apoptotic cells and the activity of caspase-3 in *HER2* amplification-positive breast cancer cells with a *PIK3CA* mutation. With the use of siRNAs specific for PIK3CA mRNA,

we further showed that survivin expression is regulated by the PI3K signaling pathway, consistent with previous studies linking survivin expression to this signaling pathway (McKenzie *et al.*, 2010; Peirce *et al.*, 2010). Our finding that survivin downregulation through inhibition of PI3K signaling was associated with the induction of apoptosis, is consistent with the key role of this signaling pathway in cell survival. We found that lapatinib downregulated survivin expression in association with the induction of apoptosis in *HER2* amplification-positive cells without an activating *PIK3CA* mutation. In contrast, expression of survivin was not markedly affected by lapatinib in cells harboring such a *PIK3CA* mutation. We therefore examined the effect of inhibition of survivin expression on lapatinib-induced apoptosis in *PIK3CA* mutant cells. In such cells, the combination of survivin depletion by RNAi and lapatinib treatment exhibited a pro-apoptotic effect markedly greater than that observed with either approach alone, suggesting that downregulation of survivin promotes lapatinib-induced apoptosis. We also found that, unlike lapatinib, the PI3K inhibitor BEZ235 induced downregulation of survivin expression in cells with an activating *PIK3CA* mutation, suggesting that this effect contributes, at least in part, to the enhanced level of apoptosis induced by the combination of lapatinib and BEZ235. Insufficient inhibition of the PI3K-survivin pathway may thus account for the smaller pro-apoptotic effect of lapatinib in *HER2* amplification-positive cells with an activating *PIK3CA* mutation compared with that observed in those without such a mutation.

In conclusion, we have shown that both induction of BIM and inhibition of survivin have a role in lapatinib-induced apoptosis in *HER2* amplification-positive breast cancer cells. Moreover, both the PI3K-survivin pathway and the MEK-ERK-BIM pathway contribute independently to the induction of apoptosis in these cells regardless of *PIK3CA* mutational status. Our data thus show that simultaneous interruption of the PI3K-survivin and MEK-ERK-BIM pathways is required for effective induction of apoptosis in breast cancer cells with *HER2* amplification. They further provide a rationale for the development of new therapeutic strategies for patients with breast tumors positive for *HER2* amplification, including those with an activating *PIK3CA* mutation.

Materials and methods

Cell culture and reagents

The human breast cancer cell lines SK-BR3, ZR-75-30, BT-474, MB-361, MB-453, HCC1954, MCF-7, T47-D and MB-231 were obtained from American Type Culture Collection (Manassas, VA, USA). SK-BR3 cells were cultured in McCoy's medium (Invitrogen, Carlsbad, CA, USA) supplemented with 10% fetal bovine serum; BT-474 cells in Dulbecco's modified Eagle's medium (Invitrogen) supplemented with 10% fetal bovine serum; MB-361, MB-453 and MB-231 cells in L15 medium (Invitrogen) supplemented with 10% fetal bovine serum; and the remaining cells in RPMI 1640 medium (Sigma, St Louis, MO, USA) supplemented with 10% fetal bovine serum. All cells were maintained under a humidified atmosphere of 5% CO_2 at 37 °C. Lapatinib was obtained from Sequoia Research Products (Pangbourne, UK), AZD6244 was from ShangHai Biochempartner (Shanghai, China) and LY294002 and U0126 were from Cell Signaling Technology (Danvers, MA, USA). BEZ235 was kindly provided by Novartis (Basel, Switzerland). MB-453 and HCC1954 cells were found to harbor an H1047 hotspot mutation, and MB-361 cells were found to contain an E545K hotspot mutation by sequencing of exons 9 and 20 of *PIK3CA* (Hoeflich *et al.*, 2009; Kataoka *et al.*, 2010; Saal *et al.*, 2005; Samuels *et al.*, 2004). We categorized BT-474 cells as negative for an activating *PIK3CA* mutation for this study on the basis of the demonstrated lack of transforming activity for the K111N mutation and its minimal effect on downstream signaling (Gymnopoulos *et al.*, 2007; Zhang *et al.*, 2008).

Growth inhibition assay in vitro

Cells were plated in 96-well flat-bottomed plates and cultured for 24 h before exposure to various concentrations of lapatinib for 72 h. TetraColor One (5 mM tetrazolium monosodium salt and 0.2 mM 1-methoxy-5-methyl phenazinium methylsulfate; Seikagaku, Tokyo, Japan) was then added to each well, and the cells were incubated for 3 h at 37 °C before measurement of absorbance at 490 nm with a Multiskan Spectrum instrument (Thermo Labsystems, Boston, MA, USA). Absorbance values were expressed as a percentage of that for untreated cells, and the concentration of lapatinib resulting in 50% growth inhibition (IC_{50}) was calculated.

Annexin V binding assay

Binding of annexin V to cells was measured with the use of an Annexin-V-FLUOS Staining Kit (Roche, Basel, Switzerland). Cells were harvested by exposure to trypsin-EDTA, washed with phosphate-buffered saline and centrifuged at 200 *g* for 5 min. The cell pellets were resuspended in 100 μl of Annexin-V-FLUOS labeling solution, incubated for 10–15 min at 15–25 °C and then analyzed for fluorescence with a flow cytometer (FACSCalibur) and Cell Quest software (Becton Dickinson, Franklin Lakes, NJ, USA).

Clonogenicity assay

Cells were seeded in triplicate in six-well plates and cultured for 48 h in the presence of lapatinib (1 μM) or vehicle. They were then cultured in drug-free medium for 14 days, fixed with methanol:acetic acid (10:1, v/v) and stained with crystal violet. The mean percentage cell survival relative to controls was determined from triplicate wells.

Immunoblot analysis

Cells were washed twice with ice-cold phosphate-buffered saline and then lysed in a solution containing 20 mM Tris-HCl (pH 7.5), 150 mM NaCl, 1 mM EDTA, 1% Triton X-100, 2.5 mM sodium pyrophosphate, 1 mM phenylmethylsulfonyl fluoride and leupeptin (1 μg/ml). The protein concentration of cell lysates was determined with a BCA protein assay kit (Thermo Fischer Scientific, Waltham, MA, USA), and equal amounts of protein were subjected to SDS–polyacrylamide gel electrophoresis on a 7.5 or 12% gel (Bio-Rad, Hercules, CA, USA). The separated proteins were transferred to a nitrocellulose membrane, which was then incubated with Blocking One solution (Nacalai Tesque, Kyoto, Japan) for 20 min at room temperature before incubation overnight at 4 °C with primary antibodies. Rabbit polyclonal antibodies to human phosphorylated HER2 (pY1248), to phosphorylated AKT, to

AKT, to BIM, to Mcl-1, to Bcl-2, to Bcl-x_L, to XIAP and to p110α were obtained from Cell Signaling Technology; those to phosphorylated ERK and to ERK were from Santa Cruz Biotechnology (Santa Cruz, CA, USA); those to c-IAP1 were from R&D Systems (Minneapolis, MN, USA); those to HER2 were from Millipore (Billerica, MA, USA); those to survivin were from Novus (Littleton, CO, USA); and those to β-actin were from Sigma. All antibodies were used at a 1:1000 dilution, with the exception of those to β-actin (1:200). The membrane was then washed with phosphate-buffered saline containing 0.05% Tween 20 before incubation for 1 h at room temperature with horseradish peroxidase-conjugated goat antibodies to rabbit immunoglobulin G (Sigma). Immune complexes were finally detected with chemiluminescence reagents (GE Healthcare, Little Chalfont, UK).

Gene silencing
Cells were plated at 50–60% confluence in six-well plates or 25-cm^2 flasks and then incubated for 24 h before transient transfection for the indicated times with siRNAs mixed with the Lipofectamine reagent (Invitrogen). The siRNAs specific for PIK3CA (PIK3CA-1, 5′-UCAACUUCUUCAAGAUG AA-3′; PIK3CA-2, 5′-GUAGAAUGUUUACUACCAA-3′), BIM (BIM-1, 5′-GGAGGGUAUUUUUGAAUAA-3′; BIM-2, 5′-AGGAGGGUAUUUUUGAAUA-3′), or survivin (survivin-1, 5′-GAAGCAGUUUGAAGAAUUA-3′; survivin-2, 5′-AGAAGCAGUUUGAAGAAUU-3′) mRNAs as well as non-specific (control) siRNAs were obtained from Nippon EGT (Toyama, Japan).

Assay of caspase-3 activity
The activity of caspase-3 in cell lysates was measured with the use of a CCP32/Caspase-3 Fluometric Protease Assay Kit (MBL, Woburn, MA, USA). Fluorescence attributable to cleavage of the Asp–Glu–Val–Asp–7-amino-4-trifluoromethyl coumarin (DEVD-AFC) substrate was measured at excitation and emission wavelengths of 390 and 460 nm, respectively.

Growth inhibition assay in vivo
All animal studies were done with the Recommendations for Handling of Laboratory Animals for biochemical Research compiled by the Committee on Safety and Ethical Handling Regulations for Laboratory Animal Experiments, Kinki University. Cubic fragments of tumor tissue (~2 by 2 by 2 mm) formed by HCC1954 cells were implanted subcutaneously into the axilla of 5–6-week-old male athymic nude mice. When their tumors became palpable, mice were divided in to four groups and treated with vehicle, BEZ235 alone, lapatinib alone and the combination of BEZ235 and lapatinib. Each treatment group contained six mice. BEZ235 and lapatinib were administered by oral gavage daily for 14 days; control animals received a 0.5% (w/v) aqueous solution of hydroxypropylmethylcellulose as vehicle. Tumor volume was determined from caliper measurements of tumor length (L) and width (W) according to the formula $LW^2/2$. Both tumor size and body weight were measured twice per week.

Statistical analysis
Quantitative data from *in vitro* experiments are presented as means ± s.e. from three independent experiments, and were analyzed with the unpaired two-tailed Student's t-test. *In vivo* data are presented as means ± s.e. from six mice and were analyzed by the unpaired two-tailed Student's t-test. A P-value of <0.05 was considered statistically significant.

Conflict of interest

The authors declare no conflict of interest.

Acknowledgements

We thank E Hatashita, K Kuwata, and H Yamaguchi for technical assistance.

References

Altieri DC. (2003). Validating survivin as a cancer therapeutic target. *Nat Rev Cancer* **3**: 46–54.

Ambrosini G, Adida C, Altieri DC. (1997). A novel anti-apoptosis gene, survivin, expressed in cancer and lymphoma. *Nat Med* **3**: 917–921.

Berns K, Horlings HM, Hennessy BT, Madiredjo M, Hijmans EM, Beelen K *et al.* (2007). A functional genetic approach identifies the PI3K pathway as a major determinant of trastuzumab resistance in breast cancer. *Cancer Cell* **12**: 395–402.

Brachmann SM, Hofmann I, Schnell C, Fritsch C, Wee S, Lane H *et al.* (2009). Specific apoptosis induction by the dual PI3K/mTor inhibitor NVP-BEZ235 in HER2 amplified and PIK3CA mutant breast cancer cells. *Proc Natl Acad Sci USA* **106**: 22299–22304.

Burris III HA, Taylor CW, Jones SF, Koch KM, Versola MJ, Arya N *et al.* (2009). A phase I and pharmacokinetic study of oral lapatinib administered once or twice daily in patients with solid malignancies. *Clin Cancer Res* **15**: 6702–6708.

Chen L, Willis SN, Wei A, Smith BJ, Fletcher JI, Hinds MG *et al.* (2005). Differential targeting of prosurvival Bcl-2 proteins by their BH3-only ligands allows complementary apoptotic function. *Mol Cell* **17**: 393–403.

Costa DB, Halmos B, Kumar A, Schumer ST, Huberman MS, Boggon TJ *et al.* (2007). BIM mediates EGFR tyrosine kinase inhibitor-induced apoptosis in lung cancers with oncogenic EGFR mutations. *PLoS Med* **4**: 1669–1679; discussion 1680.

Cragg MS, Jansen ES, Cook M, Harris C, Strasser A, Scott CL. (2008). Treatment of B-RAF mutant human tumor cells with a MEK inhibitor requires Bim and is enhanced by a BH3 mimetic. *J Clin Invest* **118**: 3651–3659.

Cragg MS, Kuroda J, Puthalakath H, Huang DC, Strasser A. (2007). Gefitinib-induced killing of NSCLC cell lines expressing mutant EGFR requires BIM and can be enhanced by BH3 mimetics. *PLoS Med* **4**: 1681–1689; discussion 1690.

Di Leo A, Gomez HL, Aziz Z, Zvirbule Z, Bines J, Arbushites MC *et al.* (2008). Phase III, double-blind, randomized study comparing lapatinib plus paclitaxel with placebo plus paclitaxel as first-line treatment for metastatic breast cancer. *J Clin Oncol* **26**: 5544–5552.

Eichhorn PJ, Gili M, Scaltriti M, Serra V, Guzman M, Nijkamp W *et al.* (2008). Phosphatidylinositol 3-kinase hyperactivation results in lapatinib resistance that is reversed by the mTOR/phosphatidylinositol 3-kinase inhibitor NVP-BEZ235. *Cancer Res* **68**: 9221–9230.

Geyer CE, Forster J, Lindquist D, Chan S, Romieu CG, Pienkowski T *et al.* (2006). Lapatinib plus capecitabine for HER2-positive advanced breast cancer. *N Engl J Med* **355**: 2733–2743.

Gomez HL, Doval DC, Chavez MA, Ang PC, Aziz Z, Nag S *et al.* (2008). Efficacy and safety of lapatinib as first-line therapy for ErbB2-amplified locally advanced or metastatic breast cancer. *J Clin Oncol* **26**: 2999–3005.

Gong Y, Somwar R, Politi K, Balak M, Chmielecki J, Jiang X *et al.* (2007). Induction of BIM is essential for apoptosis triggered by EGFR kinase inhibitors in mutant EGFR-dependent lung adenocarcinomas. *PLoS Med* **4**: e294.

Gymnopoulos M, Elsliger MA, Vogt PK. (2007). Rare cancer-specific mutations in PIK3CA show gain of function. *Proc Natl Acad Sci USA* **104**: 5569–5574.

Hoeflich KP, O'Brien C, Boyd Z, Cavet G, Guerrero S, Jung K *et al.* (2009). *in vivo* antitumor activity of MEK and phosphatidylinositol 3-kinase inhibitors in basal-like breast cancer models. *Clin Cancer Res* **15**: 4649–4664.

Isakoff SJ, Engelman JA, Irie HY, Luo J, Brachmann SM, Pearline RV *et al.* (2005). Breast cancer-associated PIK3CA mutations are oncogenic in mammary epithelial cells. *Cancer Res* **65**: 10992–11000.

Kanwar JR, Shen WP, Kanwar RK, Berg RW, Krissansen GW. (2001). Effects of survivin antagonists on growth of established tumors and B7-1 immunogene therapy. *J Natl Cancer Inst* **93**: 1541–1552.

Kataoka Y, Mukohara T, Shimada H, Saijo N, Hirai M, Minami H. (2010). Association between gain-of-function mutations in PIK3CA and resistance to HER2-targeted agents in HER2-amplified breast cancer cell lines. *Ann Oncol* **21**: 255–262.

Konecny GE, Pegram MD, Venkatesan N, Finn R, Yang G, Rahmeh M *et al.* (2006). Activity of the dual kinase inhibitor lapatinib (GW572016) against HER-2-overexpressing and trastuzumab-treated breast cancer cells. *Cancer Res* **66**: 1630–1639.

LoRusso PM, Jones SF, Koch KM, Arya N, Fleming RA, Loftiss J *et al.* (2008). Phase I and pharmacokinetic study of lapatinib and docetaxel in patients with advanced cancer. *J Clin Oncol* **26**: 3051–3056.

McKenzie JA, Liu T, Goodson AG, Grossman D.. (2010). Survivin enhances motility of melanoma cells by supporting Akt activation and {alpha}5 inte. *Cancer Res* **70**: 7927–7937.

Olie RA, Simoes-Wust AP, Baumann B, Leech SH, Fabbro D, Stahel RA *et al.* (2000). A novel antisense oligonucleotide targeting survivin expression induces apoptosis and sensitizes lung cancer cells to chemotherapy. *Cancer Res* **60**: 2805–2809.

Peirce SK, Findley HW, Prince C, Dasgupta A, Cooper T, Durden DL. (2010). The PI-3 kinase-Akt-MDM2-survivin signaling axis in high-risk neuroblastoma: a target for PI-3 kinase inhibitor intervention. *Cancer Chemother Pharmacol* (e-pub ahead of print 24 October 2010; DOI:10.1007/s00280-1010-1486-7).

Saal LH, Holm K, Maurer M, Memeo L, Su T, Wang X *et al.* (2005). PIK3CA mutations correlate with hormone receptors, node metastasis, and ERBB2, and are mutually exclusive with PTEN loss in human breast carcinoma. *Cancer Res* **65**: 2554–2559.

Samuels Y, Wang Z, Bardelli A, Silliman N, Ptak J, Szabo S *et al.* (2004). High frequency of mutations of the PIK3CA gene in human cancers. *Science* **304**: 554.

Serra V, Markman B, Scaltriti M, Eichhorn PJ, Valero V, Guzman M *et al.* (2008). NVP-BEZ235, a dual PI3K/mTOR inhibitor, prevents PI3K signaling and inhibits the growth of cancer cells with activating PI3K mutations. *Cancer Res* **68**: 8022–8030.

Slamon DJ. (1990). Studies of the HER-2/neu proto-oncogene in human breast cancer. *Cancer Invest* **8**: 253.

Slamon DJ, Clark GM, Wong SG, Levin WJ, Ullrich A, McGuire WL. (1987). Human breast cancer: correlation of relapse and survival with amplification of the HER-2/neu oncogene. *Science* **235**: 177–182.

Slamon DJ, Godolphin W, Jones LA, Holt JA, Wong SG, Keith DE *et al.* (1989). Studies of the HER-2/neu proto-oncogene in human breast and ovarian cancer. *Science* **244**: 707–712.

Speliotes EK, Uren A, Vaux D, Horvitz HR. (2000). The survivin-like C. elegans BIR-1 protein acts with the Aurora-like kinase AIR-2 to affect chromosomes and the spindle midzone. *Mol Cell* **6**: 211–223.

Stemke-Hale K, Gonzalez-Angulo AM, Lluch A, Neve RM, Kuo WL, Davies M *et al.* (2008). An integrative genomic and proteomic analysis of PIK3CA, PTEN, and AKT mutations in breast cancer. *Cancer Res* **68**: 6084–6091.

Tanaka K, Iwamoto S, Gon G, Nohara T, Iwamoto M, Tanigawa N. (2000). Expression of survivin and its relationship to loss of apoptosis in breast carcinomas. *Clin Cancer Res* **6**: 127–134.

Toi M, Iwata H, Fujiwara Y, Ito Y, Nakamura S, Tokuda Y *et al.* (2009). Lapatinib monotherapy in patients with relapsed, advanced, or metastatic breast cancer: efficacy, safety, and biomarker results from Japanese patients phase II studies. *Br J Cancer* **101**: 1676–1682.

Uren AG, Wong L, Pakusch M, Fowler KJ, Burrows FJ, Vaux DL *et al.* (2000). Survivin and the inner centromere protein INCENP show similar cell-cycle localization and gene knockout phenotype. *Curr Biol* **10**: 1319–1328.

Zhang H, Liu G, Dziubinski M, Yang Z, Ethier SP, Wu G. (2008). Comprehensive analysis of oncogenic effects of PIK3CA mutations in human mammary epithelial cells. *Breast Cancer Res Treat* **112**: 217–227.

Zhao JJ, Liu Z, Wang L, Shin E, Loda MF, Roberts TM. (2005). The oncogenic properties of mutant p110alpha and p110beta phosphatidylinositol 3-kinases in human mammary epithelial cells. *Proc Natl Acad Sci USA* **102**: 18443–18448.

Supplementary Information accompanies the paper on the Oncogene website (http://www.nature.com/onc)

A Novel Mass Spectrometry–Based Assay for Diagnosis of *EML4-ALK*–Positive Non–Small Cell Lung Cancer

Kazuko Sakai, PhD, Isamu Okamoto, MD, PhD,† Ken Takezawa, MD, PhD,† Tomonori Hirashima, MD,‡ Hiroyasu Kaneda, MD, PhD,† Masayuki Takeda, MD, PhD,† Kazuko Matsumoto, MD, PhD,* Hideharu Kimura, MD, PhD,* Yoshihiko Fujita, PhD,* Kazuhiko Nakagawa, MD, PhD,† Tokuzo Arao, MD, PhD,* and Kazuto Nishio, MD, PhD**

Introduction: The presence of the transforming fusion gene echinoderm microtubule-associated protein–like 4 (*EML4*)–anaplastic lymphoma kinase (*ALK*) in non–small-cell lung cancer (NSCLC) is a predictive marker for the efficacy of anaplastic lymphoma kinase inhibitors. However, the currently available assays for the detection of the different variants of *EML4-ALK* have limitations.

Methods: We developed an assay system for the detection of *EML4-ALK* variants 1, 2, 3a, 3b, 4, 5a, 5b, 6, or 7 transcripts in total RNA obtained from formalin-fixed, paraffin-embedded (FFPE) specimens of NSCLC tissue. The assay is based on region-specific polymerase chain reaction amplification of *EML4-ALK* complementary DNA followed by specific single-base primer extension and analysis of the extension products by matrix-assisted laser desorption/ionization–time of flight mass spectrometry. The assay was validated by fluorescence in situ hybridization and the results confirmed by subcloning and sequencing of polymerase chain reaction products.

Results: Evaluation of the analytic sensitivity of the assay with serial dilutions of plasmids containing *EML4-ALK* complementary DNA sequences revealed it to be capable of the reliable detection of one copy of each plasmid per reaction. The assay also detected *EML4-ALK* variants 1 or 3 in three FFPE samples of surgically resected NSCLC shown to be positive for anaplastic lymphoma kinase rearrangement by fluorescence in situ hybridization. Furthermore, the assay identified variant 1 of *EML4-ALK* in 3 of 20 FFPE biopsy samples from patients with advanced NSCLC. All positive samples were confirmed by subcloning and sequencing.

Conclusions: Our novel assay is highly sensitive and effective for the detection of *EML4-ALK* in FFPE specimens.

Key Words: EML4-ALK, Non–small cell lung cancer, Paraffin-embedded tissue, Mass spectrometry, Diagnosis.

(*J Thorac Oncol.* 2012;7: 913–918)

*Department of Genome Biology and †Department of Medical Oncology, Kinki University, Faculty of Medicine, Osaka-Sayama, Osaka, Japan; and ‡Department of Thoracic Malignancy, Osaka Prefectural Medical Center for Respiratory and Allergic Diseases, Habikino-shi, Osaka, Japan.

Conflict of interest: The authors declare no conflict of interest.

Address for correspondence: Kazuto Nishio, MD, PhD, Kinki University Faculty of Medicine, Ohnohigashi 377-2, Osaka-sayama, Osaka, Japan. E-mail: knishio@med.kindai.ac.jp

ISSN: 1556-0864/12/913-918

Echinoderm microtubule-associated protein–like 4 (EML4)–anaplastic lymphoma kinase (ALK) was recently identified as a transforming fusion protein in lung cancer.[1] Both *EML4* and *ALK* genes are located on the short arm of chromosome 2. Multiple variants of *EML4-ALK* have been identified, with all variants including the same cytoplasmic portion of ALK but different portions of EML4 (with truncations at exons 2, 6, 13, 14, 15, 18, and 20).[2–4] The most common *EML4-ALK* variants are 1 and 3, which together account for ~60% of *EML4-ALK*–positive cases of non–small cell lung cancer (NSCLC).[5] Crizotinib, an inhibitor of the tyrosine kinase activity of ALK and MET (hepatocyte growth factor receptor), has been shown to be effective for the treatment of lung cancer patients harboring *EML4-ALK*.[6] Indeed, crizotinib was recently approved by the U.S. Food and Drug Administration for the treatment of advanced NSCLC in patients with an abnormal *ALK* gene.

The *EML4-ALK* translocation occurs in 5 to 10% of lung cancer patients.[1,2,7–10] Several assays have been developed for the detection of this translocation in clinical samples.[2,4,11] However, all of these assays have limitations with regard to sensitivity or the reliance on specialized techniques, with the development of higher-sensitivity assays based on simple methods being warranted.

MATERIALS AND METHODS

Plasmid Construction

Plasmids based on pCR2.1 or pcDNA3.1(+) and containing *EML4-ALK* or *ALK* complementary DNA (cDNA) were constructed as positive controls by TA cloning (Invitrogen, Madison, WI) or In-Fusion PCR cloning (Clontech, Palo Alto, CA).[12] Details of plasmid construction and corresponding primer sequences are provided in Supplemental Digital Content 1 (http://links.lww.com/JTO/A219) and 2 (http://links.lww.com/JTO/A220).

Clinical Samples

Formalin-fixed, paraffin-embedded (FFPE) samples were obtained from NSCLC patients who had undergone surgery or biopsy for the purpose of diagnosis at Kinki University Hospital. The study was approved by the Institutional Review Board with the conditions that samples

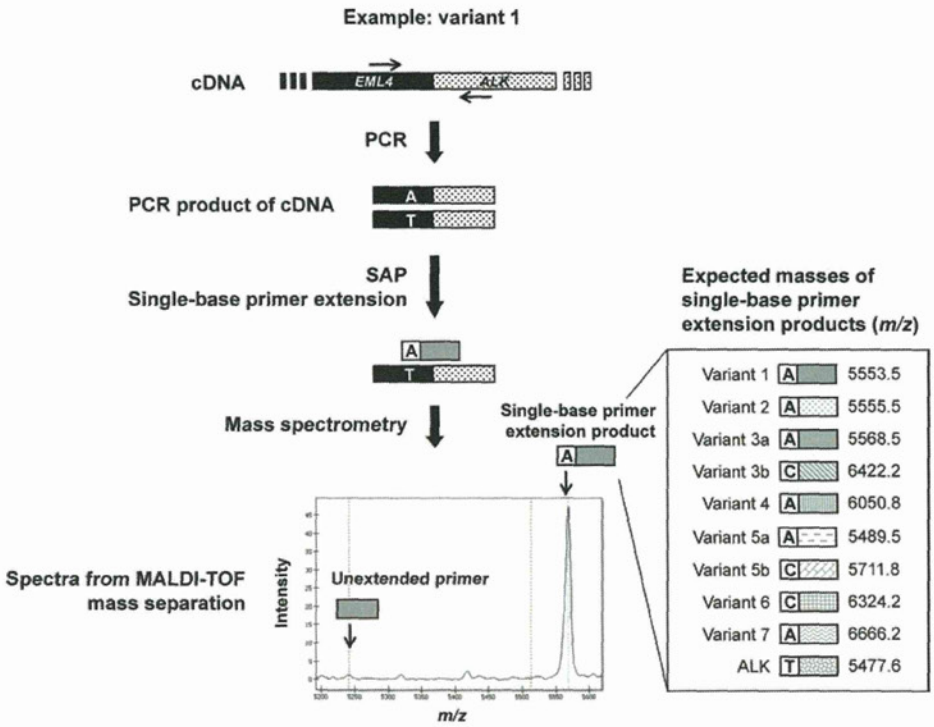

FIGURE 1. MassARRAY method for the detection of *EML4-ALK*. The region of *EML4-ALK* complementary DNA containing the fusion point is amplified by polymerase chain reaction (PCR), with the amplicons ranging in size from 70 to 130 bp. After dephosphorylation of the 5′ terminus of the PCR products with the use of shrimp alkaline phosphatase, a single-base primer extension reaction is performed. The primer extension products are then analyzed by matrix-assisted laser desorption ionization–time of flight mass spectrometry . The single-base extension reaction occurs only when an *EML4-ALK* fusion product is present in the sample.

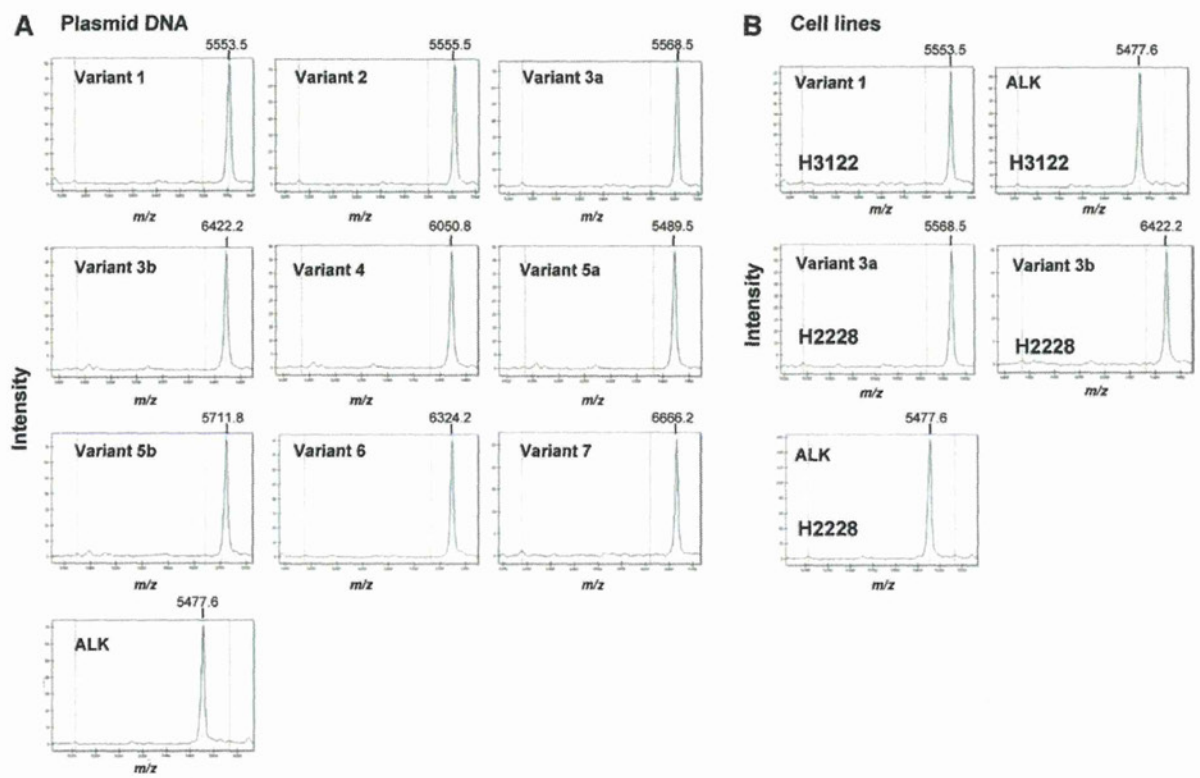

FIGURE 2. Representative spectra for *EML4-ALK* variants. Plasmid DNA (1 ng per reaction) containing the indicated variants of *EML4-ALK* (*A*) or total complementary DNA (5 ng per reaction) prepared from H3122 or H2228 cell lines (which harbor *EML4-ALK* variant 1 and variants 3a and 3b, respectively) (*B*) was subjected to the MassARRAY assay. Representative spectra for extension products between ~5100 and ~6800 Da are shown. The expected *m/z* values for each single-base extension product are as indicated in Figure 1. Three independent experiments were performed in triplicate with identical results.

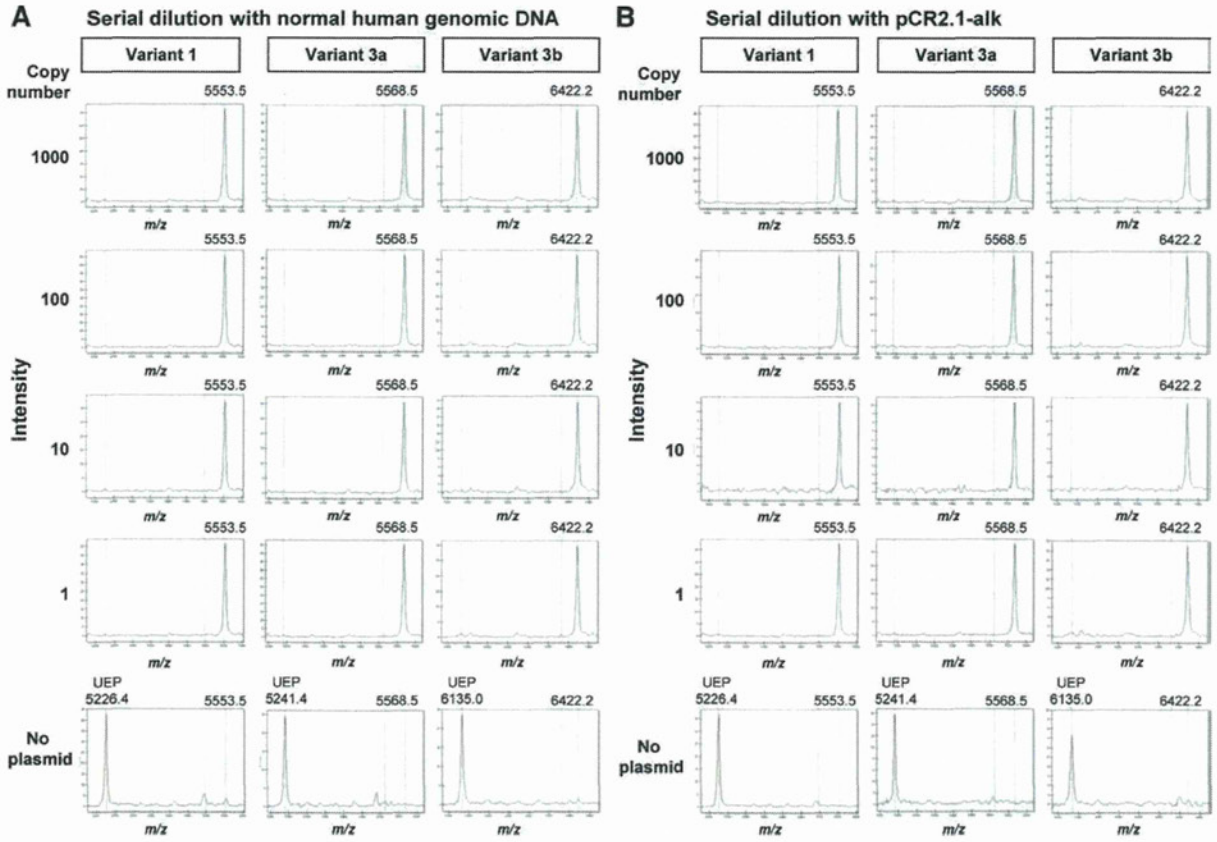

FIGURE 3. Sensitivity of *EML4-ALK* detection in plasmid DNA. The indicated copy numbers of pcDNA3.1(+) containing variants 1, 3a, or 3b of *EML4-ALK* were assayed in the presence of 1 ng of normal human genomic DNA (*A*) or 10 pg of pCR2.1-alk plasmid DNA (*B*). The copy number of plasmid DNA per reaction was calculated according to the formula: $6.022 \times 10^{23} \times$ [mass of DNA (g)]/[plasmid size (bp) $\times$ 660]. Three independent experiments were performed in triplicate with identical results. UEP, unextended primer.

be processed anonymously and analyzed for gene expression and that the study be disclosed publicly, according to the Ethical Guidelines for Human Genome Research published by the Ministry of Education, Culture, Sports, Science, and Technology, the Ministry of Health, Labor, and Welfare, and the Ministry of Economy, Trade, and Industry of Japan. The study also conforms to the provisions of the Declaration of Helsinki.

Cell Lines

The human NSCLC cell lines H2228 and H3122 were kindly provided by Dr. P. A. Jänne (Department of Medical Oncology, Dana-Farber Cancer Institute, Boston, MA). Short tandem repeat analysis was performed with genomic DNA isolated from H2228 and H3122 cells. The DNA profile of H2228 cells matched that in the American Type Culture Collection short tandem repeat database. The cells were maintained under a humidified atmosphere of 5% CO_2 at 37°C in RPMI 1640 medium (Sigma, St. Louis, MO) supplemented with 10% heat-inactivated fetal bovine serum (Equitech-Bio, Kerrville, TX).

Sample Processing

Total RNA was extracted from cell lines and FFPE samples with the use of an RNeasy Mini Kit (Qiagen, Valencia, CA) and an RNeasy FFPE Kit (Qiagen), respectively. The percentage of tumor cells in each FFPE specimen was evaluated by hematoxylin-eosin staining and found to be >10%. The isolated RNA was subjected to reverse transcription (RT) with the use of a High Capacity cDNA Reverse Transcription Kit (Applied Biosystems, Foster City, CA), and the resulting cDNA was stored at –80°C until analysis.

Detection of *EML4-ALK*

We used the MassARRAY iPLEX platform (Sequenom, San Diego, CA) for detection of *EML4-ALK*. The MassARRAY system involves a three-step process consisting of polymerase chain reaction (PCR), single-base primer extension, and separation of the products on a matrix-loaded silicon chip by matrix-assisted laser desorption ionization (MALDI)–time of flight (TOF) mass spectrometry (MS) (Fig. 1). PCR and the single-base primer extension reactions were performed in a thermal cycler (ABI-9700 instrument, Applied Biosystems), and the extension products were analyzed using the MALDI–TOF MS

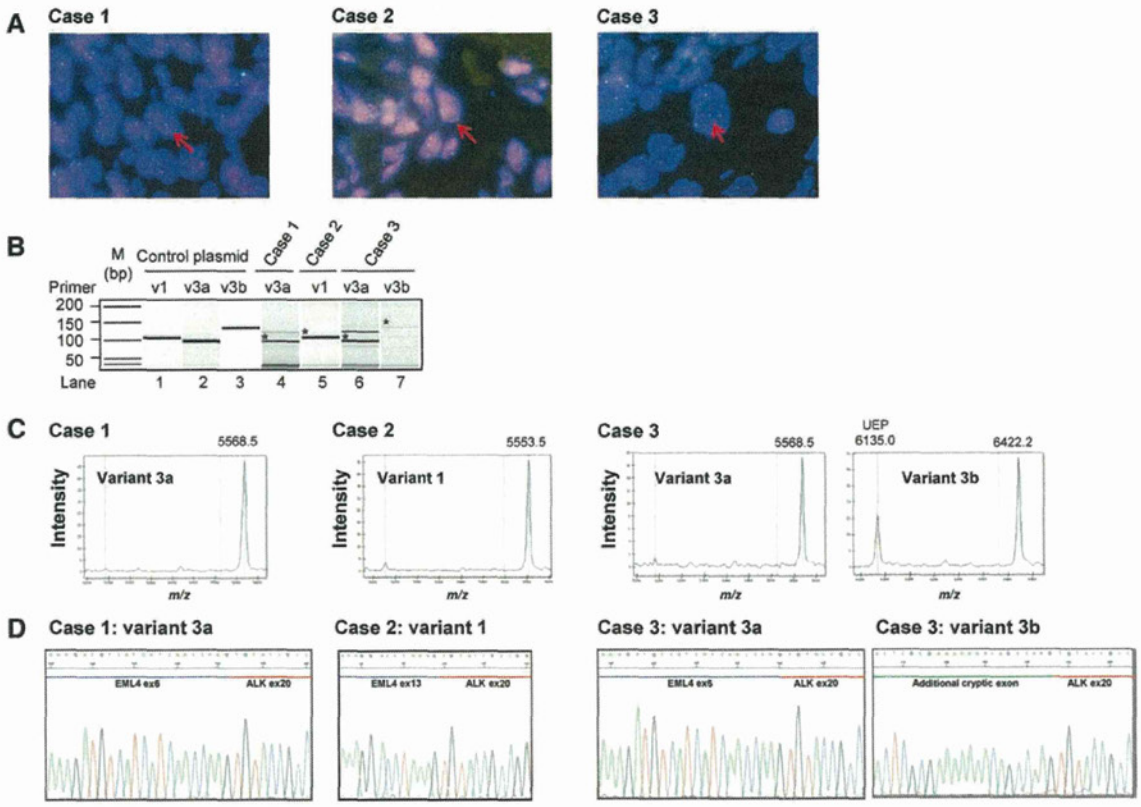

FIGURE 4. Detection of *EML4-ALK* in formalin-fixed, paraffin-embedded (FFPE) samples of surgically resected non–small cell lung cancer tissue. (*A*) Clinical specimens were subjected to fluorescence in situ hybridization analysis with differentially labeled probes for the 5′ (green) or 3′ (red) regions of the *ALK* locus. A pair of split signals (arrows) indicates the rearranged *ALK* locus. (*B*) polymerase chain reaction (PCR) products derived with PCR primer sets in the MassARRAY assay were separated with the use of an Agilent 2100 Bioanalyzer and a DNA 1000 LabChip Kit (Agilent Technologies, Inc., Palo Alto, CA). The PCR products are from pcDNA3.1(+)-v1 (lane 1), pcDNA3.1(+)-v3a (lane 2), pcDNA3.1(+)-v3b (lane 3), case 1 (lane 4), case 2 (lane 5), and case 3 (lanes 6 and 7). The asterisk indicates the corresponding band in each case. (*C*) Total RNA (10 ng) isolated from the FFPE samples in (*A*) was analyzed by the MassARRAY assay. Representative spectra are shown. The experiment was repeated twice with identical results. (*D*) The PCR products from (*C*) were also subcloned and sequenced. ex, exon.

(Sequenom). Detailed procedures and corresponding primer sequences are provided in Supplemental Digital Content 1 (http://links.lww.com/JTO/A219) and 3 (http://links.lww.com/JTO/A221), respectively.

Sequencing Analysis

PCR products were subcloned into the TOPO TA pCR2.1 vector (Invitrogen) and sequenced with an automated sequencer (ABI Prism 3100 Genetic Analyzer, Applied Biosystems) with the use of M13 universal primers.

Fluorescence In Situ Hybridization Analysis

FFPE tissue sectioned at a thickness of 4 μm and placed on glass slides was subjected to fluorescence in situ hybridization (FISH) with a break-apart probe for the *ALK* gene (Vysis LSI ALK Dual Color, Break Apart Rearrangement Probe; Abbott Molecular, Des Plaines, IL). FISH positivity was defined as the presence of >15% split signals in tumor cells.

RESULTS

Detection of *EML4-ALK* Variants

We developed an assay system based on the MassARRAY platform for the detection of *EML4-ALK* variants in NSCLC tissue (Fig. 1). The MassARRAY assay detected plasmid DNA corresponding to nine different *EML4-ALK* variants and wild-type *ALK* (Fig. 2*A*). Appropriate mass spectra for the single-base extension products were thus obtained (Figs. 1 and 2*A*). We next attempted to detect *EML4-ALK* in the human NSCLC cell lines H3122 and H2228, which harbor *EML4-ALK* variants 1 and 3, respectively.[7] The RT-PCR products of total RNA isolated from the cell lines were subjected to the MassARRAY assay. *EML4-ALK* variant 1 was detected in H3122 cells, whereas variants 3a and 3b were detected in H2228 cells (Fig. 2*B*). Wild-type *ALK* was also detected in both cell lines.

Sensitivity of the Assay

The major variant forms of *EML4-ALK* are variants 1, 3a, and 3b, which account for ~60% of all *EML4-ALK* fusions.[7]

TABLE 1. Characteristics of Patients Screened for *EML4-ALK*

No.	Age (years)	Sex	Histology	Procedure	Smoking status	*EML4-ALK*
1	63	F	Ad	TLB	Never	Negative
2	62	M	Ad	TBLB	Current	Negative
3	74	M	Ad	TLB	Current	Negative
4	71	M	Ad	TBLB	Current	Negative
5	63	F	Ad	TBLB	Never	Variant 1
6	75	M	Ad	TBLB	Former	Negative
7	59	M	Ad	Needle biopsy	Current	Negative
8	85	M	Ad	TBLB	Current	Negative
9	73	F	Ad	Lymph node biopsy	Never	Negative
10	68	F	Ad	TBLB	Current	Negative
11	65	M	Ad	TBLB	Current	Variant 1
12	57	M	Ad	TBLB	Current	Negative
13	68	F	Ad	TLB	Never	Negative
14	73	M	Ad	TBLB	Former	Negative
15	67	F	Ad	TBLB	Never	Negative
16	67	M	Ad	TBLB	Former	Negative
17	57	M	Ad	TBLB	Former	Negative
18	56	M	Large	TBLB	Current	Negative
19	65	M	Ad	TBLB	Current	Negative
20	60	M	Ad	TBLB	Current	Variant 1

Ad, adenocarcinoma; Large, large cell carcinoma; TLB, thoracoscopic lung biopsy; TBLB, transbronchial lung biopsy.

We therefore examined the sensitivity of our assay for detection of these variants. Samples containing 1000, 100, 10, or 1 copy of plasmid DNA [pcDNA3.1(+) for variants 1, 3a, or 3b] and 1 ng of normal human genomic DNA (Promega, Madison, WI) were prepared by 10-fold serial dilution. MS spectra revealed a clear peak at the expected size for variants 1, 3a, or 3b in all samples, including those containing only one copy of the variant DNA (Fig. 3*A*). We also examined assay sensitivity when the samples were diluted with pCR2.1 containing *ALK* cDNA (pCR2.1-alk). Samples containing 1000, 100, 10, or 1 copy of the variant plasmids were thus diluted with 10 pg (~2 × 10^6 copies) of pCR2.1-alk. A clear peak at the expected size was again detected in all the samples including those containing only one copy of the variant DNA (Fig. 3*B*). These results therefore suggested that the sensitivity of the assay for the detection of *EML4-ALK* variants is high.

Detection of *EML4-ALK* Variants in FFPE Samples

We next evaluated the ability of our assay to detect *EML4-ALK* variants in three surgically resected FFPE samples of NSCLC shown to be positive for *ALK* rearrangements by FISH analysis (Fig. 4*A*). The primary PCR products for the assay were also analyzed by gel electrophoresis, with the expected sizes of the amplification products being 115, 103, and 119 bp for variants 1, 3a, and 3b, respectively. Bands corresponding to *EML4-ALK* variant 1 (case 2), variant 3a (cases 1 and 3), and variant 3b (case 3) were detected (Fig. 4*B*). Similarly, we detected MS peaks corresponding to *EML4-ALK* variant 1 and to variants 3a or 3b in case 2 and in cases 1 and 3, respectively (Fig. 4*C*). The presence of *EML4-ALK* variants in these three cases was confirmed by subcloning and sequencing of PCR products (Fig. 4*D*). We further analyzed several NSCLC specimens shown to be negative for *EML4-ALK* by FISH analysis; no mass peaks for *EML4-ALK* variants were detected by the MassARRAY assay (data not shown). These results thus suggested that the MassARRAY assay is able to detect *EML4-ALK* variants in FFPE samples.

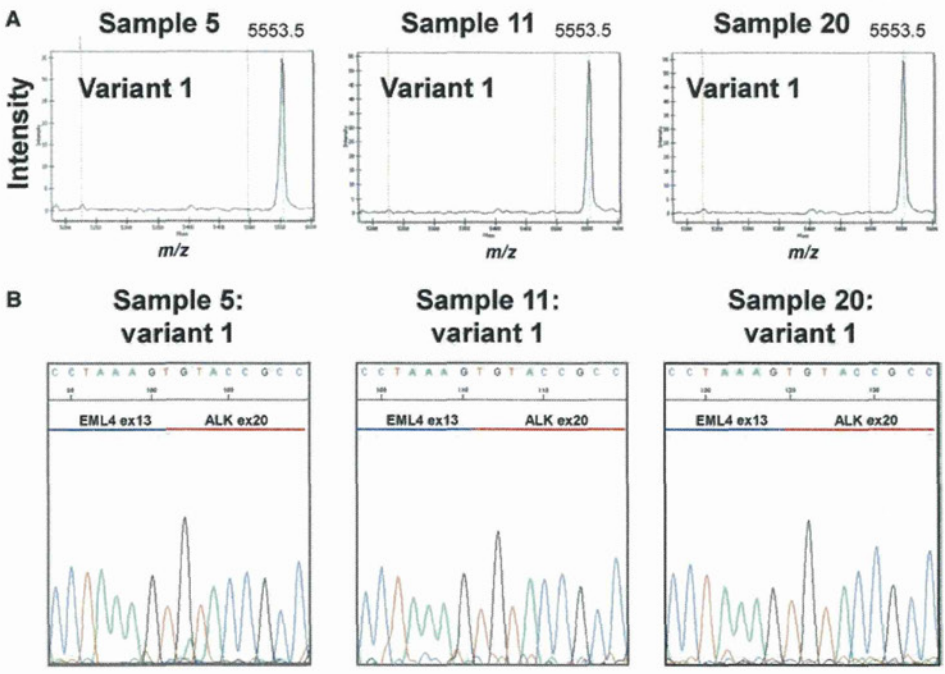

FIGURE 5. Detection of *EML4-ALK* in formalin-fixed, paraffin-embedded samples of non–small cell lung cancer obtained by transbronchial lung biopsy. (*A*) Representative spectra of *EML4-ALK*–positive samples. The experiments were repeated twice with identical results. (*B*) The polymerase chain reaction products from (*A*) were subcloned and sequenced.

Screening for *EML4-ALK* Variants in FFPE Biopsy Samples of Advanced NSCLC

Molecular analysis of biopsy samples from patients with advanced NSCLC is often difficult because of the small amount of tissue available. We therefore examined the feasibility of detection of *EML4-ALK* variants with the MassARRAY assay in FFPE biopsy specimens obtained from 20 patients with advanced NSCLC, the characteristics of whom are shown in Table 1. Three specimens (samples 5, 11, and 20) were found to be positive for variant 1 of *EML4-ALK*, with none of the other variants being detected (Fig. 5*A*). The presence of *EML4-ALK* variant 1 in these three cases was confirmed by subcloning and sequencing of PCR products (Fig. 5*B*). We also performed FISH analysis on the 20 FFPE specimens. Of the three *EML4-ALK*–positive cases detected by the MassARRAY assay, two (samples 5 and 20) were positive by FISH whereas the third (sample 11) could not be evaluated because of poor tissue quality (data not shown). None of the cases that tested negative by the MassARRAY assay was positive by FISH. These results thus suggested that our assay is effective for *EML4-ALK* screening with FFPE biopsy specimens of advanced NSCLC.

DISCUSSION

We have developed a MassARRAY assay for screening of *EML4-ALK* in FFPE samples of NSCLC tissue. This novel assay is capable of detecting nine different *EML4-ALK* variants with a high sensitivity.

Dual-color split-signal FISH analysis has been considered the gold standard in screening for *ALK* rearrangement. However, given that *EML4* and *ALK* loci are located in relatively close proximity on chromosome 2p, the detection of the *EML4-ALK* fusion gene on the basis of the gap between the probes is sometimes difficult. The identification and counting of signals on tissue sections is impeded by factors such as cutting artifacts and nuclear overlap related to the thickness and homogeneity of the tissue sections and the size of the nuclei. The MassARRAY system is a nucleic acid analysis platform which utilizes a three-step process composed of PCR amplification, single-base primer extension, and MALDI–TOF MS analysis. The presence of *EML4-ALK* in our MassARRAY assay is detected on the basis of the presence of products of predicted mass.

The amount of tumor tissue available for molecular analysis is often limited in patients with advanced NSCLC. Furthermore, RNA extracted from FFPE samples is highly degraded and less amenable to RT-PCR analysis compared with that isolated from nonfixed, freshly frozen tissue. We succeeded in amplifying *EML4-ALK* cDNA by PCR from FFPE tissue with primers designed to yield short amplicons (70–130 bp). The design of such short amplicons can also be applied to quantitative PCR systems such as amplification-refractory mutation system for allele-specific PCR assays. In our system, PCR amplification was performed with a high number of cycles (45 cycles), and increased accumulation of PCR products conferred higher sensitivity. We tested 20 FFPE biopsy samples from patients with NSCLC with our assay and detected a clear mass peak for *EML4-ALK* variant 1 in 3 of these samples, each of which was confirmed positive for this variant by subcloning and sequencing of the PCR products. In contrast to FISH, our assay is able to distinguish between the different *EML4-ALK* variants in a small amount of FFPE NSCLC tissue, and it should prove to be a useful tool for the detection of *EML4-ALK* variants in diagnostic testing for this fusion gene.

ACKNOWLEDGMENTS

Supported by the Third-Term Comprehensive 10-Year Strategy for Cancer Control of the Ministry of Education, Culture, Sports, Science, and Technology of Japan as well as by Health and Labor Scientific Research Grants [20-9].

REFERENCES

1. Soda M, Choi YL, Enomoto M, et al. Identification of the transforming EML4-ALK fusion gene in non-small-cell lung cancer. *Nature* 2007;448:561–566.
2. Takeuchi K, Choi YL, Soda M, et al. Multiplex reverse transcription-PCR screening for EML4-ALK fusion transcripts. *Clin Cancer Res* 2008;14:6618–6624.
3. Choi YL, Takeuchi K, Soda M, et al. Identification of novel isoforms of the EML4-ALK transforming gene in non-small cell lung cancer. *Cancer Res* 2008;68:4971–4976.
4. Takeuchi K, Choi YL, Togashi Y, et al. KIF5B-ALK, a novel fusion oncokinase identified by an immunohistochemistry-based diagnostic system for ALK-positive lung cancer. *Clin Cancer Res* 2009;15:3143–3149.
5. Sasaki T, Rodig SJ, Chirieac LR, Jänne PA. The biology and treatment of EML4-ALK non-small cell lung cancer. *Eur J Cancer* 2010;46:1773–1780.
6. Kwak EL, Bang YJ, Camidge DR, et al. Anaplastic lymphoma kinase inhibition in non-small-cell lung cancer. *N Engl J Med* 2010;363:1693–1703.
7. Koivunen JP, Mermel C, Zejnullahu K, et al. EML4-ALK fusion gene and efficacy of an ALK kinase inhibitor in lung cancer. *Clin Cancer Res* 2008;14:4275–4283.
8. Inamura K, Takeuchi K, Togashi Y, et al. EML4-ALK fusion is linked to histological characteristics in a subset of lung cancers. *J Thorac Oncol* 2008;3:13–17.
9. Wong DW, Leung EL, So KK, et al.; University of Hong Kong Lung Cancer Study Group. The EML4-ALK fusion gene is involved in various histologic types of lung cancers from nonsmokers with wild-type EGFR and KRAS. *Cancer* 2009;115:1723–1733.
10. Martelli MP, Sozzi G, Hernandez L, et al. EML4-ALK rearrangement in non-small cell lung cancer and non-tumor lung tissues. *Am J Pathol* 2009;174:661–670.
11. Rodig SJ, Mino-Kenudson M, Dacic S, et al. Unique clinicopathologic features characterize ALK-rearranged lung adenocarcinoma in the western population. *Clin Cancer Res* 2009;15:5216–5223.
12. Takezawa K, Okamoto I, Nishio K, Jänne PA, Nakagawa K. Role of ERK-BIM and STAT3-survivin signaling pathways in ALK inhibitor-induced apoptosis in EML4-ALK-positive lung cancer. *Clin Cancer Res* 2011;17:2140–2148.

Published OnlineFirst July 27, 2012; DOI: 10.1158/1078-0432.CCR-12-0392

Clinical Cancer Research

Activation of HER Family Signaling as a Mechanism of Acquired Resistance to ALK Inhibitors in EML4-ALK –Positive Non–Small Cell Lung Cancer

Junko Tanizaki, Isamu Okamoto, Takafumi Okabe, et al.

Clin Cancer Res 2012;18:6219-6226. Published OnlineFirst July 27, 2012.

Published OnlineFirst July 27, 2012; DOI: 10.1158/1078-0432.CCR-12-0392

Cancer Therapy: Preclinical

Clinical Cancer Research

Activation of HER Family Signaling as a Mechanism of Acquired Resistance to ALK Inhibitors in EML4-ALK–Positive Non–Small Cell Lung Cancer

Junko Tanizaki[1], Isamu Okamoto[1], Takafumi Okabe[3], Kazuko Sakai[2], Kaoru Tanaka[1], Hidetoshi Hayashi[1], Hiroyasu Kaneda[1], Ken Takezawa[1], Kiyoko Kuwata[1], Haruka Yamaguchi[1], Erina Hatashita[1], Kazuto Nishio[2], and Kazuhiko Nakagawa[1]

Abstract

Purpose: Anaplastic lymphoma kinase (ALK) tyrosine kinase inhibitors (TKI) such as crizotinib show marked efficacy in patients with non–small cell lung cancer positive for the echinoderm microtubule-associated protein–like 4 (EML4)–ALK fusion protein. However, acquired resistance to these agents has already been described in treated patients, and the mechanisms of such resistance remain largely unknown.

Experimental Design: We established lines of EML4-ALK–positive H3122 lung cancer cells that are resistant to the ALK inhibitor TAE684 (H3122/TR cells) and investigated their resistance mechanism with the use of immunoblot analysis, ELISA, reverse transcription and real-time PCR analysis, and an annexin V binding assay. We isolated EML4-ALK–positive lung cancer cells (K-3) from a patient who developed resistance to crizotinib and investigated their characteristics.

Results: The expression of EML4-ALK was reduced at the transcriptional level, whereas phosphorylation of epidermal growth factor receptor (EGFR), HER2, and HER3 was upregulated, in H3122/TR cells compared with those in H3122 cells. This activation of HER family proteins was accompanied by increased secretion of EGF. Treatment with an EGFR-TKI induced apoptosis in H3122/TR cells, but not in H3122 cells. The TAE684-induced inhibition of extracellular signal–regulated kinase (ERK) and STAT3 phosphorylation observed in parental cells was prevented by exposure of these cells to exogenous EGF, resulting in a reduced sensitivity of cell growth to TAE684. K-3 cells also manifested HER family activation accompanied by increased EGF secretion.

Conclusions: EGF-mediated activation of HER family signaling is associated with ALK-TKI resistance in lung cancer positive for EML4-ALK. *Clin Cancer Res; 18(22); 6219–26. ©2012 AACR.*

Introduction

Lung cancer is the leading cause of cancer death worldwide. Fusion of the echinoderm microtubule-associated protein–like 4 gene (*EML4*) with the anaplastic lymphoma kinase gene (*ALK*), which results in the production of a fusion protein (EML4-ALK), occurs in 5% to 10% of cases of non–small cell lung cancer (NSCLC; refs. 1–3). This transforming fusion leads to activation of downstream signaling molecules, and inhibition of ALK signaling has shown marked antitumor effects in NSCLC positive for EML4-ALK in both preclinical and clinical studies (4). Despite their initial response, however, individuals with EML4-ALK–positive NSCLC treated with ALK inhibitors eventually acquire resistance to these drugs (5), and the molecular mechanisms responsible for such resistance remain largely uncharacterized. With the use of an *in vitro* cell model and cells newly derived from a patient with acquired resistance to the ALK inhibitor crizotinib, we have now uncovered a previously unknown mechanism of such resistance.

Authors' Affiliations: Departments of [1]Medical Oncology and [2]Genome Biology, Kinki University Faculty of Medicine, Osaka-Sayama, Osaka; and [3]National Hospital Organization Minamiwakayama Medical Center, Tanabe, Wakayama, Japan

Note: Supplementary data for this article are available at Clinical Cancer Research Online (http://clincancerres.aacrjournals.org/).

Corresponding Author: Isamu Okamoto, Department of Medical Oncology, Kinki University Faculty of Medicine, 377-2 Ohno-higashi, Osaka-Sayama, Osaka 589-8511, Japan. Phone: 81-72-366-0221; Fax: 81-72-360-5000; E-mail: chi-okamoto@dotd.med.kindai.ac.jp

doi: 10.1158/1078-0432.CCR-12-0392

Materials and Methods

Cell culture and reagents

The H3122 human NSCLC cell line was obtained as previously described (6), and H1299 human NSCLC cells were obtained from American Type Culture Collection. The cells were maintained under a humidified atmosphere of 5% CO_2 at 37°C in RPMI 1640 medium (Sigma), which contains no biologic ligands including EGF, supplemented with 10% FBS. TAE684, crizotinib, and BIBW2992 were obtained from ShangHai Biochempartner. Paclitaxel was from Sigma, and adriamycin was from Wako. Recombinant

Published OnlineFirst July 27, 2012; DOI: 10.1158/1078-0432.CCR-12-0392

Translational Relevance

ALK-targeted therapy shows marked clinical efficacy in lung cancer patients with the *EML4-ALK* fusion gene. Such patients eventually develop resistance to ALK tyrosine kinase inhibitors (TKI), however, and the mechanisms of such resistance remain largely unknown. We have now established ALK-TKI–resistant lines of *EML4-ALK*–positive H3122 cells and shown that activation of the epidermal growth factor receptor (EGFR) and the related proteins HER2 and HER3 by autocrine EGF stimulation is associated with such resistance. Furthermore, we established K-3 cells from a specimen of *EML4-ALK*–positive lung cancer obtained from a patient who developed ALK-TKI resistance. These cells also manifested EGF-dependent activation of HER family proteins. Our observations have thus uncovered a previously unknown mechanism of ALK-TKI resistance in *EML4-ALK*–positive lung cancer and they may provide a basis for circumvention of such resistance.

human epidermal growth factor (EGF) was from R&D Systems.

Generation of TAE684-resistant H3122 cells

H3122 cells were initially exposed to 0.01 μmol/L TAE684. They were then isolated by limiting dilution, maintained, and passaged normally with gradually increasing doses of TAE684, up to a maximum of 1 μmol/L. The established resistant cell lines, designated H3122/TR1 and H3122/TR2, were maintained in medium containing the maximal dose of TAE684 (1 μmol/L) to maintain selective pressure for TAE684 resistance.

Growth inhibition assay *in vitro*

Cell viability was assessed with an MTT assay as previously described (7).

Annexin V binding assay

Binding of annexin V to cells was measured with the use of an Annexin-V-FLUOS Staining Kit (Roche), as previously described (7).

Immunoblot analysis

Immunoblot analysis was conducted as previously described (7). Rabbit polyclonal antibodies to phosphorylated human ALK (pY1608), to ALK, to the phosphorylated EGF receptor (pY1068), to phosphorylated HER2 (pY1221), to phosphorylated HER3 (pY1289), to phosphorylated AKT, to AKT, to phosphorylated STAT3, and to STAT3 were obtained from Cell Signaling Technology; those to HER3, to extracellular signal-regulated kinase (ERK), and to phosphorylated ERK were from Santa Cruz Biotechnology; those to HER2 were from Millipore; and those to β-actin were from Sigma. Mouse monoclonal antibodies to the EGF receptor (EGFR) were obtained from Invitrogen.

Reverse transcription and real-time PCR analysis

Total RNA was extracted from cells with the use of an RNeasy Mini Kit (Qiagen) and was subjected to reverse transcription (RT) with the use of a SuperScript Preamplification System (Invitrogen Life Technologies). The resulting cDNA was then subjected to real-time PCR analysis with the use of a One Step SYBR PrimeScript RT-PCR Kit (Takara Bio) and ABI PRISM 7900HT system (Applied Biosystems). The PCR primers (forward and reverse, respectively) included those for EML4-ALK (5′-GTGCAGTGTTTAGCATTCTTGGGG-3′, 5′-TCTTGCCAGCAAAGCAGTAGTTGG-3′), EGF (5′-TGCAACTGTGTTGTTGGCTACATC-3′, 5′-TGGTTGACCCCCATTCTTGAG-3′), TGF-α (5′-TCAGTTCTGCTTCCATGCAACC-3′, 5′-TTTCTGAGTGGCAGCAAGCG-3′), and amphiregulin (5′-AGAGTTGAACAGGTAGTTAAGCCCC-3′, 5′-GTCGAAGTTTCTTTCGTTCCTCAG-3′). Glyceraldehyde-3-phosphate dehydrogenase (GAPDH) mRNA was used as an internal standard.

ELISA for ligands

The concentrations of EGF, TGF-α, and amphiregulin in conditioned medium were determined as previously described (8), with the use of a Human Quantikine ELISA Kit (R&D Systems).

Isolation of crizotinib-resistant cells from a clinical specimen

K-3 cells were established at Kinki University Faculty of Medicine from the pleural effusion of a patient with EML4-ALK–positive NSCLC who developed resistance to crizotinib. The cells were cultured in Dulbecco's modified Eagle's medium supplemented with 10% FBS. The clinical specimen was obtained from Kinki University Hospital for study with the approval of the Institutional Review Board, and the patient provided written informed consent.

Results

Generation of ALK inhibitor–resistant lines from EML4-ALK–positive H3122 cells

The NSCLC cell line H3122 expresses EML4-ALK and is highly sensitive to the ALK TKI TAE684. We generated TAE684-resistant H3122 cell lines (H3122/TR1 and H3122/TR2) by exposing the parental cells to increasing

Table 1. IC_{50} values of TAE684 and crizotinib for inhibition of the growth of H3122 and H3122/TR cell lines

	IC50, μmol/L	
Cell line	TAE684	Crizotinib
H3122	0.053	0.15
H3122/TR1	1.034	2.26
H3122/TR2	1.100	1.51

NOTE: Data are means of triplicates from representative experiments that were repeated a total of 3 times.

Published OnlineFirst July 27, 2012; DOI: 10.1158/1078-0432.CCR-12-0392

concentrations of TAE684. Short tandem repeat analysis of H3122/TR cells confirmed their H3122 origin (data not shown). The IC_{50} of TAE684 for inhibition of the growth of the parental H3122 cells was 0.053 μmol/L, whereas those for the H3122/TR cell lines as well as for EML4-ALK–negative H1299 cells were all more than 1 μmol/L (Table 1, Fig. 1A). The H3122/TR cells were also resistant to crizotinib, another ALK-targeted TKI, but not to other drugs including paclitaxel and adriamycin (Table 1, Fig. 1A, and data not shown). TAE684 also induced a marked increase in the level of apoptosis in H3122 cells, whereas it had no such effect in H3122/TR cells (Fig. 1B). Collectively, these data suggested that H3122/TR cells had acquired resistance specific to ALK inhibitors.

Activation of alternative signaling pathways in H3122/TR cells

We next investigated the mechanism responsible for resistance to ALK-TKIs in H3122/TR cells. Immunoblot analysis revealed that the abundance of EML4-ALK was reduced in both H3122/TR cell lines compared with that in H3122 cells (Fig. 2A). Quantitative RT-PCR analysis showed that the amount of EML4-ALK mRNA was also reduced markedly in H3122/TR cells relative to that in the parental cells (Supplementary Fig. 1), suggesting that the downregulation of EML4-ALK expression is mediated at the transcriptional level. We did not detect any secondary mutations of ALK in H3122/TR cells (data not shown), with such mutations having previously been shown to give rise to ALK-TKI resistance (5, 9, 10). TAE684 inhibited the phosphorylation of ERK and STAT3 in H3122 cells, but had no such effects in H3122/TR cells (Fig. 2A). Given that signaling via ERK and STAT3 is maintained in H3122/TR cells in the presence of TAE684, we investigated whether alternative upstream pathways are activated in these cells. We found that the level of EGFR phosphorylation was increased in the resistant cells compared with the parental cells, although the abundance of EGFR was decreased in the former cells (Fig. 2B). Phosphorylation of the EGFR-related proteins HER2 and HER3 was also increased in both H3122/TR cell lines (Fig. 2B). To investigate the mechanism responsible for activation of these receptor tyrosine kinases in H3122/TR cells, we examined the expression of ligands for HER family proteins, including EGF, TGF-α, and amphiregulin. Quantitative RT-PCR analysis revealed that the amount of EGF mRNA, but not that of TGF-α or amphiregulin mRNAs, was greatly increased in H3122/TR cells compared with that in parental H3122 cells (Fig. 2C). Consistent with these results, ELISA showed that secretion of EGF, but not that of TGF-α or amphiregulin, was increased in H3122/TR cells (Fig. 2D). We next examined the effect of an EGFR-TKI on apoptosis in the parental and resistant cell lines. Treatment with BIBW2992, an irreversible TKI for EGFR, induced apoptosis in H3122/TR cells, but not in H3122 cells (Fig. 2E). Furthermore, the extent of apoptosis induced by the combination of TAE684 and BIBW2992 in H3122/TR cells

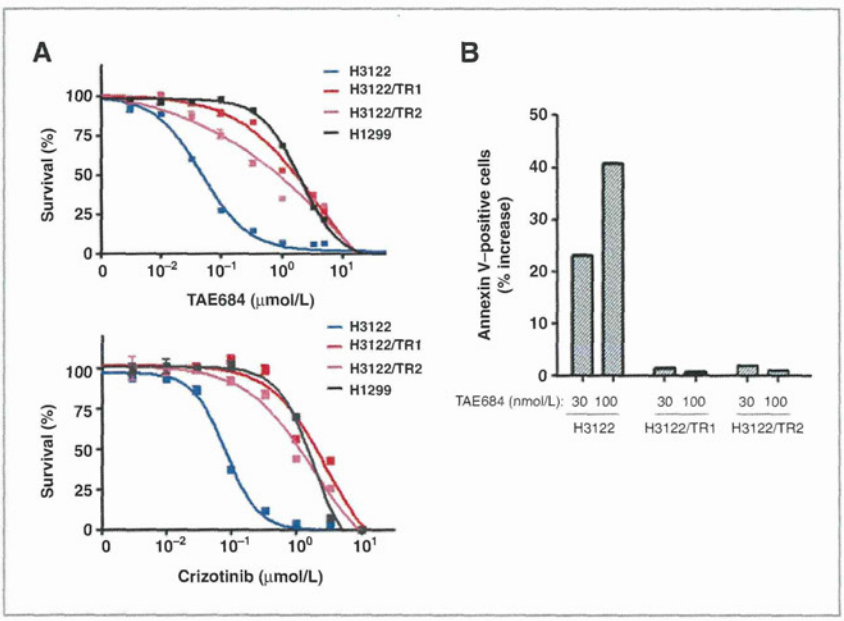

Figure 1. Effects of ALK kinase inhibitors on cell proliferation and apoptosis in H3122, H3122/TR1, H3122/TR2, and H1299 cells. A, cells were cultured for 72 hours in complete medium containing various concentrations of TAE684 (upper panel) or crizotinib (lower panel), after which cell viability was assessed. Data are means of triplicates from representative experiments and are expressed as percentage survival. B, cells were incubated for 72 hours with or without TAE684 (30 or 100 nmol/L), after which the number of apoptotic cells was determined by staining with annexin V and propidium iodide followed by flow cytometry. Data are means of triplicates from representative experiments.

Published OnlineFirst July 27, 2012; DOI: 10.1158/1078-0432.CCR-12-0392

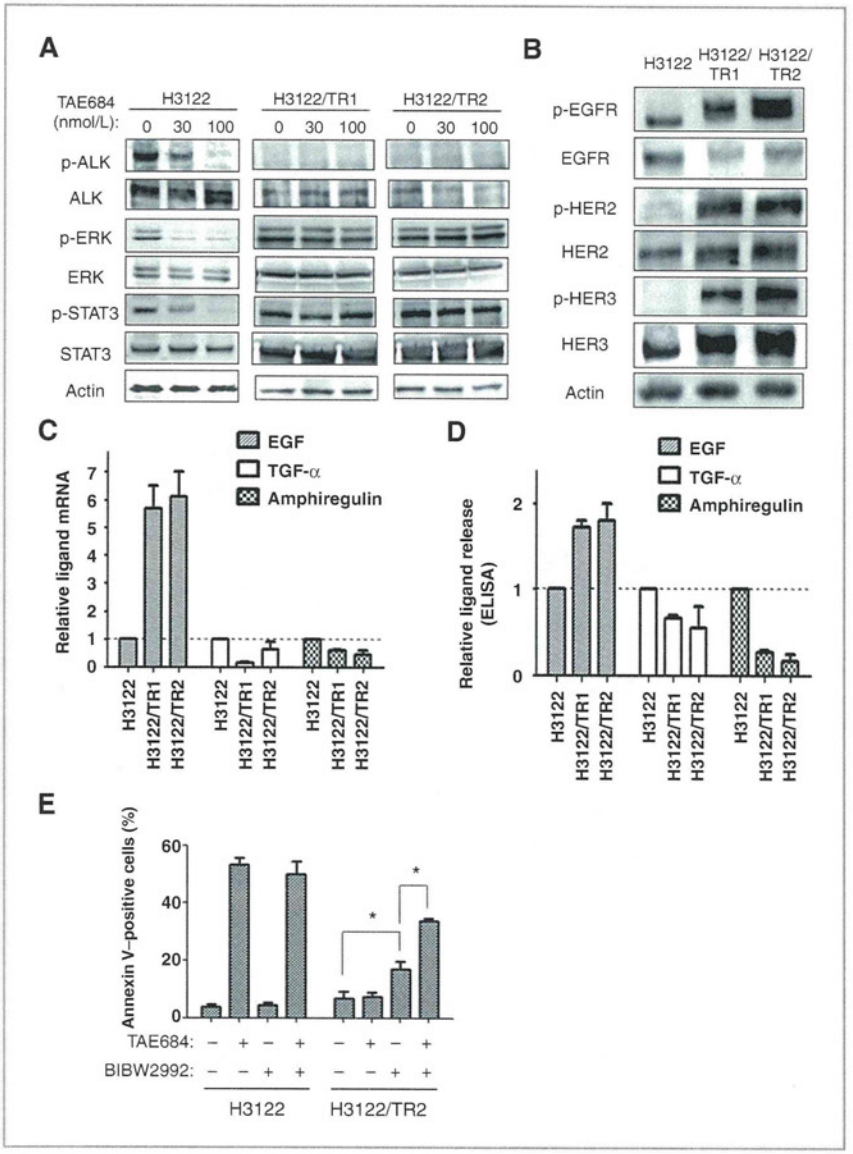

Figure 2. Activation of alternative signaling pathways in H3122/TR cells. A, H3122 or H3122/TR cells were incubated with the indicated concentrations of TAE684 for 6 hours, after which cell lysates were subjected to immunoblot analysis with antibodies to phosphorylated (p) or total forms of ALK, ERK, or STAT3 as well as with those to β-actin (loading control). B, cells were deprived of serum for 24 hours, lysed, and subjected to immunoblot analysis with antibodies to phosphorylated or total forms of EGFR, HER2, or HER3. C, total RNA extracted from the indicated cell lines was subjected to RT and real-time PCR analysis of EGF, TGF-α, and amphiregulin mRNAs. Data were normalized by the amount of GAPDH mRNA and then expressed relative to the corresponding value for H3122 cells, and they are means ± SE from three independent experiments. D, cells were cultured overnight in medium containing 10% FBS and then incubated for 24 hours in serum-free medium, after which the latter culture supernatants were collected and assayed for EGF, TGF-α, and amphiregulin with an ELISA. Data are expressed relative to the corresponding value for H3122 cells and are means ± SE from three independent experiments. E, cells were incubated for 48 hours in the absence or presence of TAE684 (100 nmol/L) or BIBW2992 (200 nmol/L), as indicated, after which the proportion of apoptotic cells was determined by staining with annexin V and propidium iodide followed by flow cytometry. Data are means ± SE from 3 independent experiments. *, $P < 0.05$ (Student's t test) for the indicated comparisons.

was significantly greater than that induced by BIBW2992 alone (Fig. 2E). Together, these observations thus indicated that EGFR, HER2, and HER3 are activated in H3122/TR cells, that this activation is accompanied by increased secretion of EGF, and that such HER family activation contributes, at least in part, to the survival of H3122/TR cells in the presence of TAE684.

EGF activates HER family signaling and induces TAE684 resistance in parental H3122 cells

To investigate whether EGF secretion plays a role in ALK-TKI resistance, we examined the effect of exogenous EGF on ALK-TKI sensitivity in H3122 cells. We found that exposure to EGF induces resistance to TAE684 in these cells (Fig. 3A), supporting the notion that increased secretion of this ligand can lead to the development of ALK-TKI resistance. TAE684 inhibited EML4-ALK phosphorylation in H3122 cells in the absence or presence of EGF stimulation, whereas it failed to inhibit downstream signaling including the phosphorylation of ERK and STAT3 in the presence of EGF (Fig. 3B). EGF increased the levels of EGFR, HER2, and HER3 phosphorylation in H3122 cells (Fig. 3C). These data suggested that EGF-induced activation of EGFR, HER2, and HER3 might underlie resistance to ALK inhibitors in H3122/TR cells.

Published OnlineFirst July 27, 2012; DOI: 10.1158/1078-0432.CCR-12-0392

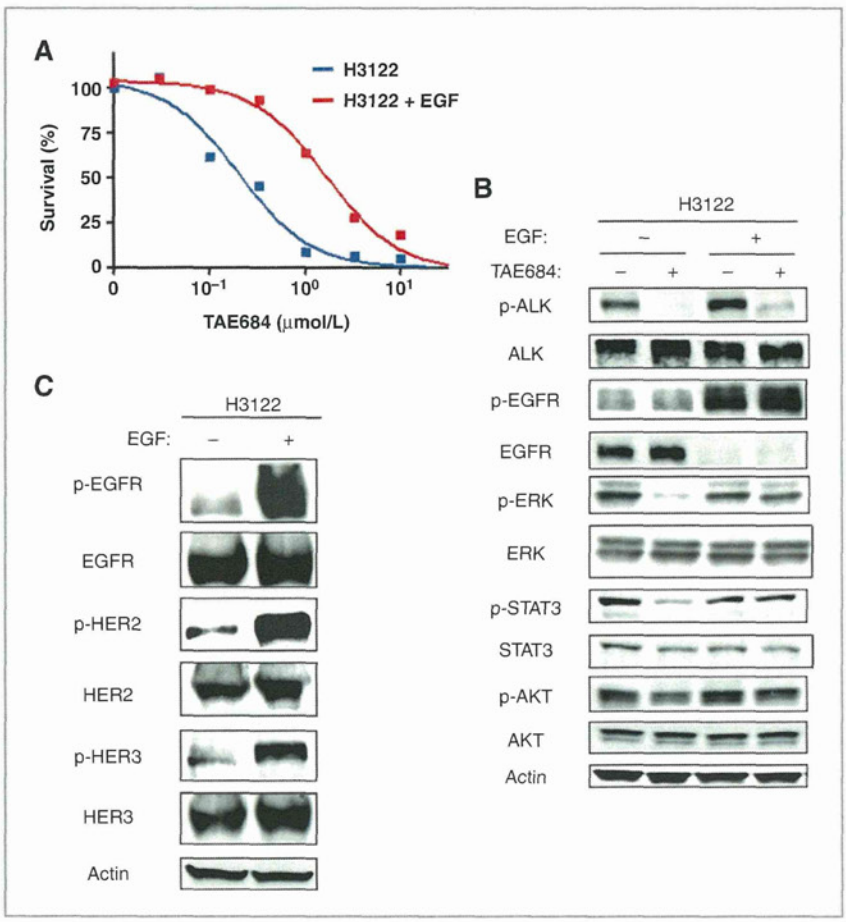

Figure 3. Effects of EGF stimulation in H3122 cells. A, cells were treated for 72 hours with various concentrations of TAE684 in the absence or presence of EGF (100 ng/mL), after which cell viability was assessed. Data are means of triplicates from representative experiments and are expressed as percentage survival. B, cells were incubated with or without EGF (100 ng/mL) for 15 min and then in the additional absence or presence of TAE684 (100 nmol/L) for 6 hours. Cell lysates were prepared and subjected to immunoblot analysis with antibodies to the indicated proteins. C, H3122 cells were incubated with or without EGF (100 ng/mL) for 6 hours, after which cell lysates were prepared and subjected to immunoblot analysis.

Isolation of drug-sensitive revertants from ALK-TKI–resistant cells

We cultured H3122/TR1 cells continuously in the absence of TAE684 for more than 2 months and thereby obtained H3122/TR revertant (H3122/TR rev) cells that had regained sensitivity to TAE684 (Fig. 4A). RT-PCR analysis and ELISA revealed that both the amount of EGF mRNA and the extent of EGF secretion in H3122/TR rev cells had been restored to levels similar to those in parental H3122 cells (Fig. 4B). This reduced level of EGF expression in H3122/TR rev cells compared with that in H3122/TR1 cells was accompanied by downregulation of EGFR, HER2, and HER3 phosphorylation as well as by upregulation of both the abundance and phosphorylation of EML4-ALK (Fig. 4C). These data suggested that downregulation of EML4-ALK expression and activation of HER family proteins, and the associated shift in signal transduction from the ALK signaling pathway to HER family pathways, are responsible for the acquired resistance to ALK inhibitors in H3122/TR cells.

Establishment of an ALK-TKI–resistant cell line from a clinical specimen

We established a cell line, designated K-3, from the pleural effusion of a patient with EML4-ALK–positive lung cancer that had developed clinical resistance to crizotinib after treatment for 6 months. The K-3 cells were found to be resistant to both crizotinib and TAE684, with IC_{50} values of 3.25 and 5.96 μmol/L, respectively (Fig. 5A). We did not detect any secondary mutations of ALK in K-3 cells. On the other hand, similar to the results obtained with H3122/TR cells, the abundance of EGF mRNA and the extent of EGF secretion were both markedly increased in K-3 cells compared with those in H3122 cells (Fig. 5B). Furthermore, immunoblot analysis showed that the level of EML4-ALK phosphorylation was decreased in K-3 cells, whereas that of EGFR, HER2, and HER3 phosphorylation was increased (Fig. 5C). These results thus showed concordance between an *in vitro* model and clinical experience of ALK-TKI resistance, further supporting the association of such resistance with EGF-dependent HER family activation.

Published OnlineFirst July 27, 2012; DOI: 10.1158/1078-0432.CCR-12-0392

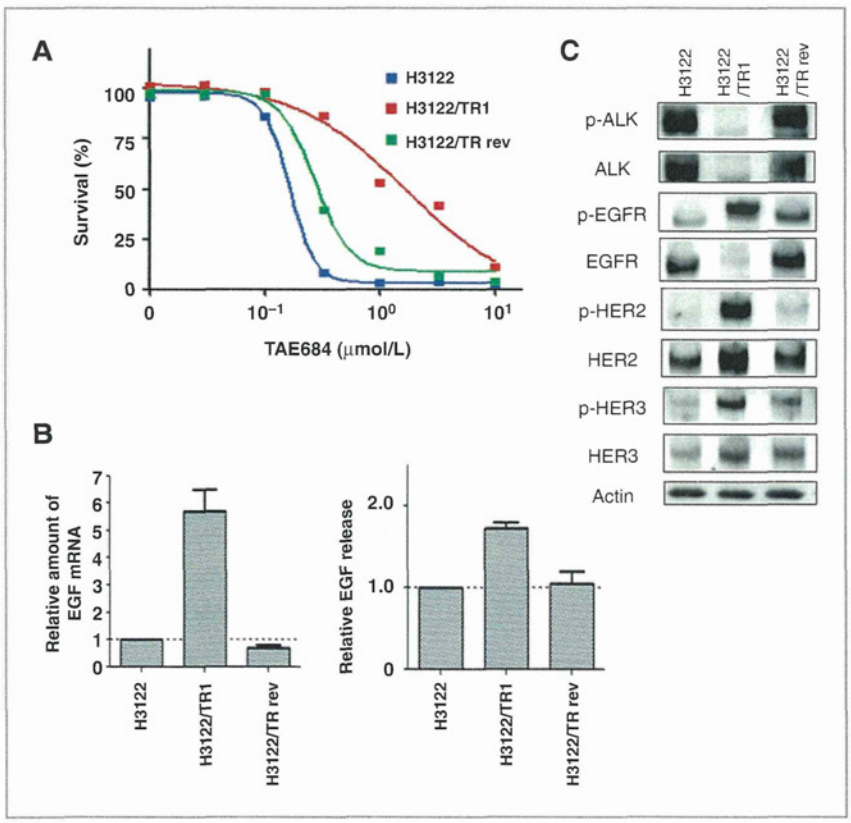

Figure 4. Characterization of H3122/TR revertant cells. A, H3122, H3122/TR1, or H3122/TR rev cells were cultured for 72 hours in complete medium containing various concentrations of TAE684, after which cell viability was assessed. Data are means of triplicates from representative experiments and are expressed as percentage survival. B, total RNA extracted from the indicated cell lines was subjected to RT and real-time PCR analysis of EGF mRNA as in Fig. 2C (left). Culture supernatants were also assayed for EGF by ELISA as in Fig. 2D (right). All data are expressed relative to the corresponding value for H3122 cells and are means ± SE from 3 independent experiments. C, cells were deprived of serum for 24 hours, after which cell lysates were prepared and subjected to immunoblot analysis with antibodies to the indicated proteins.

Discussion

EML4-ALK has been identified in 5% to 10% of NSCLC cases, and ALK-TKIs show marked antitumor effects in such tumors (3, 11, 12). However, acquired resistance to ALK inhibitors has already been found to limit the therapeutic potential of these agents (5, 10, 13), with investigation of the underlying mechanisms of such resistance thus being warranted. In the present study, we generated ALK-TKI–resistant (H3122/TR) lines from EML4-ALK–positive H3122 cells by exposing the latter sensitive cells to the ALK inhibitor TAE684, which is a more potent and selective inhibitor of ALK than is crizotinib. The H3122/TR cells were found not to harbor secondary mutations of ALK, which have previously been shown to underlie ALK-TKI resistance (5, 10, 13). Instead, we found that H3122/TR cells manifest increased activation of EGFR, HER2, and HER3 mediated by EGF as well as a reduced level of EML4-ALK activation. Such EGF-induced activation of HER family proteins was associated with sustained downstream signaling in the presence of TAE684, indicative of a shift in survival dependency from the ALK signaling pathway to HER family pathways in the ALK-TKI–resistant cells. Indeed, we found that the combination of an ALK inhibitor and an EGFR inhibitor–induced apoptosis in H3122/TR cells, further supporting the notion that the EGFR signaling pathway contributes to survival in these cells. The clinical relevance of this resistance mechanism was supported by the observation that K-3 cells, which were isolated from a specimen of EML4-ALK–positive NSCLC that developed resistance to the ALK-TKI crizotinib *in situ*, also manifested EGF-mediated HER family activation. Consistent with our results, amphiregulin-mediated EGFR activation was recently shown to be associated with resistance to ALK inhibitors (9, 14). Collectively, these data suggest that ligand-activated HER family signaling gives rise to ALK-TKI resistance. We and others have shown that ligand-mediated signaling pathway activation accompanied by upregulation of ligand mRNA is associated with resistance to molecularly targeted therapy in several cancer models (9, 15). In the present study, we found that the abundance of EGF mRNA is increased in H3122/TR cells. Given that the *EGF* gene contains consensus binding sequences for many transcription factors, including NF-κB, AP-1, AP-2, AP-3, and SP1 (16), such factors may play a role in the upregulation of EGF expression observed in our study.

In the present study, we found that, in the absence of ALK inhibition, activation of EGFR, HER2, and HER3 in H3122/TR cells becomes downregulated in association with a reversion to TAE684 sensitivity. Consistent with

Published OnlineFirst July 27, 2012; DOI: 10.1158/1078-0432.CCR-12-0392

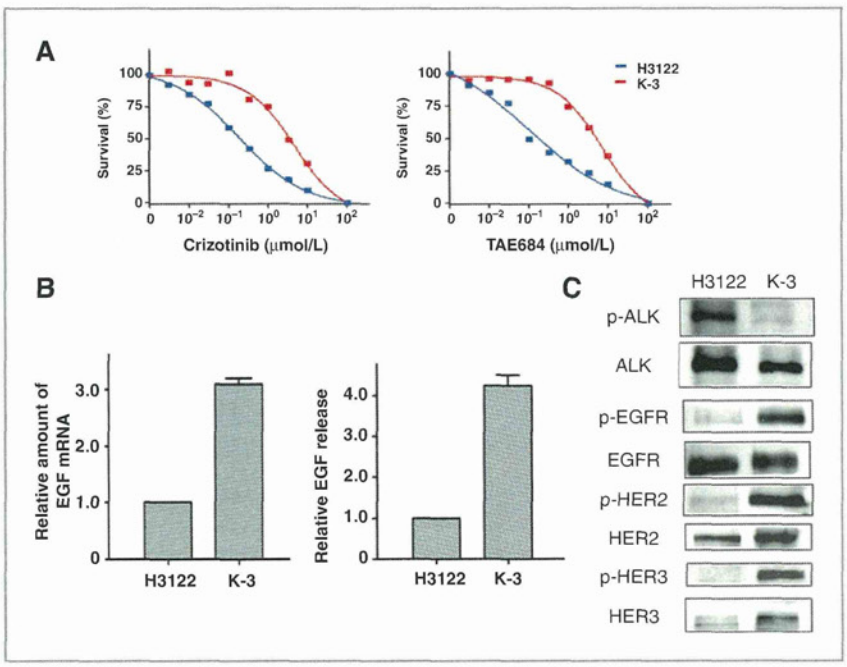

Figure 5. Characterization of K-3 cells established from a clinical specimen of EML4-ALK–positive NSCLC with acquired resistance to crizotinib. A, K-3 or H3122 cells were cultured for 72 hours in complete medium containing various concentrations of TAE684 or crizotinib, after which cell viability was assessed. Data are means of triplicates from representative experiments and are expressed as percentage survival. B, total RNA extracted from the indicated cells was subjected to RT and real-time PCR analysis of EGF mRNA as in Fig. 2C (left). Culture supernatants were also assayed for EGF by ELISA as in Fig. 2D (right). All data are expressed relative to the corresponding value for H3122 cells, and they are means ± SE from 3 independent experiments. C, cells were deprived of serum for 24 hours, after which cell lysates were prepared and subjected to immunoblot analysis with antibodies to the indicated proteins.

these results, termination of treatment with an EGFR inhibitor after the development of drug resistance in EGFR mutation–positive NSCLC resulted in the loss of the resistance-associated mutation (T790M) and restoration of tumor sensitivity to treatment with EGFR inhibitors in both preclinical and clinical settings (17–19). Our observations now suggest that the development of resistance to ALK inhibitors is potentially reversible. They provide a rationale for temporary cessation of treatment after the development of ALK-TKI resistance in patients with EML4-ALK–positive lung cancer to allow the tumor to regain drug sensitivity. Clinical evaluation of such an approach may thus be warranted.

In conclusion, with the use of *in vitro* cell lines and cells isolated from a patient, we have uncovered a previously unidentified mechanism of acquired ALK-TKI resistance in NSCLC positive for EML4-ALK. Our data add to the complexity of drug resistance mechanisms, further investigation of which is required if they are to be understood and conquered.

Disclosure of Potential Conflicts of Interest

No potential conflicts of interest were disclosed.

Authors' Contributions

Conception and design: J. Tanizaki, I. Okamoto, T. Okabe, K. Takezawa, K. Nakagawa

Development of methodology: J. Tanizaki, T. Okabe, H. Kaneda, K. Nishio

Acquisition of data (provided animals, acquired and managed patients, provided facilities, etc.): J. Tanizaki, I. Okamoto, T. Okabe, K. Sakai, K. Tanaka, H. Hayashi, K. Kuwata, H. Yamaguchi, E. Hatashita

Analysis and interpretation of data (e.g., statistical analysis, biostatistics, computational analysis): J. Tanizaki, I. Okamoto, K. Sakai, K. Kuwata, H. Yamaguchi, E. Hatashita, K. Nakagawa

Writing, review, and/or revision of the manuscript: J. Tanizaki, I. Okamoto, H. Kaneda, K. Nakagawa

Administrative, technical, or material support (i.e., reporting or organizing data, constructing databases): J. Tanizaki, K. Sakai, H. Hayashi, K. Kuwata, H. Yamaguchi, E. Hatashita

Study supervision: I. Okamoto, K. Nakagawa

The costs of publication of this article were defrayed in part by the payment of page charges. This article must therefore be hereby marked *advertisement* in accordance with 18 U.S.C. Section 1734 solely to indicate this fact.

Received February 6, 2012; revised June 9, 2012; accepted July 13, 2012; published OnlineFirst July 27, 2012.

References

1. Soda M, Choi YL, Enomoto M, Takada S, Yamashita Y, Ishikawa S, et al. Identification of the transforming EML4-ALK fusion gene in non-small-cell lung cancer. Nature 2007;448:561–6.
2. Shaw AT, Yeap BY, Mino-Kenudson M, Digumarthy SR, Costa DB, Heist RS, et al. Clinical features and outcome of patients with non-small-cell lung cancer who harbor EML4-ALK. J Clin Oncol 2009;27:4247–53.
3. Sasaki T, Rodig SJ, Chirieac LR, Janne PA. The biology and treatment of EML4-ALK non-small cell lung cancer. Eur J Cancer 2010;46:1773–80.
4. Kwak EL, Bang YJ, Camidge DR, Shaw AT, Solomon B, Maki RG, et al. Anaplastic lymphoma kinase inhibition in non-small-cell lung cancer. N Engl J Med 2010;363:1693–703.
5. Choi YL, Soda M, Yamashita Y, Ueno T, Takashima J, Nakajima T, et al. EML4-ALK mutations in lung cancer that confer resistance to ALK inhibitors. N Engl J Med 2010;363:1734–9.
6. Koivunen JP, Mermel C, Zejnullahu K, Murphy C, Lifshits E, Holmes AJ, et al. EML4-ALK fusion gene and efficacy of an ALK kinase inhibitor in lung cancer. Clin Cancer Res 2008;14:4275–83.

Published OnlineFirst July 27, 2012; DOI: 10.1158/1078-0432.CCR-12-0392

7. Tanizaki J, Okamoto I, Fumita S, Okamoto W, Nishio K, Nakagawa K. Roles of BIM induction and surviving downregulation in lapatinib-induced apoptosis in breast cancer cells with HER2 amplification. Oncogene 2011;30:4097–106.
8. Okamoto W, Okamoto I, Tanaka K, Hatashita E, Yamada Y, Kuwata K, et al. TAK-701, a humanized monoclonal antibody to hepatocyte growth factor, reverses gefitinib resistance induced by tumor-derived HGF in non-small cell lung cancer with an EGFR mutation. Mol Cancer Ther 2010;9:2785–92.
9. Sasaki T, Koivunen J, Ogino A, Yanagita M, Nikiforow S, Zheng W, et al. A novel ALK secondary mutation and EGFR signaling cause resistance to ALK kinase inhibitors. Cancer Res 2011;71:6051–60.
10. Katayama R, Khan TM, Benes C, Lifshits E, Ebi H, Rivera VM, et al. Therapeutic strategies to overcome crizotinib resistance in non-small cell lung cancers harboring the fusion oncogene EML4-ALK. Proc Natl Acad Sci USA 2011;108:7535–40.
11. Takezawa K, Okamoto I, Nishio K, Janne PA, Nakagawa K. Role of ERK-BIM and STAT3-survivin signaling pathways in ALK inhibitor-induced apoptosis in EML4-ALK-positive lung cancer. Clin Cancer Res 2011;17:2140–8.
12. Tanizaki J, Okamoto I, Takezawa K, Sakai K, Azuma K, Kuwata K, et al. Combined effect of ALK and MEK inhibitors in EML4-ALK-positive non-small-cell lung cancer cells. Br J Cancer 2012;106:763–7.
13. Sasaki T, Okuda K, Zheng W, Butrynski J, Capelletti M, Wang L, et al. The neuroblastoma-associated F1174L ALK mutation causes resistance to an ALK kinase inhibitor in ALK-translocated cancers. Cancer Res 2010;70:10038–43.
14. Katayama R, Shaw AT, Khan TM, Mino-Kenudson M, Solomon BJ, Halmos B, et al. Mechanisms of acquired crizotinib resistance in ALK-rearranged lung cancers. Sci Transl Med 2012;4:120ra17.
15. Yonesaka K, Zejnullahu K, Okamoto I, Satoh T, Cappuzzo F, Souglakos J, et al. Activation of ERBB2 signaling causes resistance to the EGFR-directed therapeutic antibody cetuximab. Sci Transl Med 2011;3:99ra86.
16. Fenton SE, Groce NS, Lee DC. Characterization of the mouse epidermal growth factor promoter and 5′-flanking region. Role for an atypical TATA sequence. J Biol Chem 1996;271:30870–8.
17. Chmielecki J, Foo J, Oxnard GR, Hutchinson K, Ohashi K, Somwar R, et al. Optimization of dosing for EGFR-mutant non-small cell lung cancer with evolutionary cancer modeling. Sci Transl Med 2011;3:90ra59.
18. Sequist LV, Waltman BA, Dias-Santagata D, Digumarthy S, Turke AB, Fidias P, et al. Genotypic and histological evolution of lung cancers acquiring resistance to EGFR inhibitors. Sci Transl Med 2011;3:75ra26.
19. Oxnard GR, Janjigian YY, Arcila ME, Sima CS, Kass SL, Riely GJ, et al. Maintained sensitivity to EGFR tyrosine kinase inhibitors in EGFR-mutant lung cancer recurring after adjuvant erlotinib or gefitinib. Clin Cancer Res 2011;17:6322–8.

Annals of Oncology

Annals of Oncology 23: 2914–2919, 2012
doi:10.1093/annonc/mds121
Published online 9 July 2012

An evaluation study of *EGFR* mutation tests utilized for non-small-cell lung cancer in the diagnostic setting

K. Goto[1*], M. Satouchi[2], G. Ishii[3], K. Nishio[4], K. Hagiwara[5], T. Mitsudomi[6], J. Whiteley[7], E. Donald[7], R. McCormack[7] & T. Todo[8]

[1]*Division of Thoracic Oncology, National Cancer Center Hospital East, Chiba;* [2]*Department of Thoracic Oncology, Hyogo Cancer Center, Hyogo;* [3]*Pathology Division, Innovative Medical Research Center, National Cancer Center Hospital East, Chiba;* [4]*Department of Genome Biology, Kinki University School of Medicine, Osaka;* [5]*Department of Respiratory Medicine, Saitama Medical University, Saitama;* [6]*Department of Thoracic Surgery, Aichi Cancer Center Hospital, Aichi, Japan;* [7]*Department of Personalised Healthcare and Biomarkers, AstraZeneca Pharmaceuticals, Macclesfield, UK;* [8]*Department of Research and Development, AstraZeneca KK, Osaka, Japan*

Received 19 December 2011; revised 2 March 2012; accepted 12 March 2012

Background: Epidermal growth factor receptor (*EGFR*) mutation is predictive for the efficacy of EGFR tyrosine kinase inhibitors in advanced non-small-cell lung cancer (NSCLC) treatment. We evaluated the performance, sensitivity, and concordance between five *EGFR* tests.

Materials and methods: DNA admixtures ($n = 34$; 1%–50% mutant plasmid DNA) and samples from NSCLC patients [116 formalin-fixed paraffin-embedded (FFPE) tissue, 29 matched bronchofiberscopic brushing (BB) cytology, and 20 additional pleural effusion (PE) cytology samples] were analyzed. *EGFR* mutation tests were PCR-Invader®, peptide nucleic acid-locked nucleic acid PCR clamp, direct sequencing, Cycleave™, and Scorpion Amplification Refractory Mutation System (ARMS)®. Analysis success, mutation status, and concordance rates were assessed.

Results: All tests except direct sequencing detected four mutation types at ≥1% mutant DNA. Analysis success rates were 91.4%–100% (FFPE) and 100% (BB and PE cytology), respectively. Inter-assay concordance rates of successfully analyzed samples were 94.3%–100% (FFPE; kappa coefficients: 0.88–1.00), 93.1%–100% (BB cytology; 0.86–1.00), and 85.0%–100% (PE cytology; 0.70–1.00), and 93.1%–96.6% (0.86–0.93) between BB cytology and matched FFPE.

Conclusions: All *EGFR* assays carried out comparably in the analysis of FFPE and cytology samples. Cytology-derived DNA is a viable alternative to FFPE samples for analyzing *EGFR* mutations.

Key words: cytology, EGFR mutation, FFPE, NSCLC, PCR

introduction

Epidermal growth factor receptor (*EGFR*) mutation is a key predictive factor for the efficacy of EGFR tyrosine kinase inhibitors in the treatment of patients with advanced non-small-cell lung cancer (NSCLC) [1–3]. *EGFR* mutation testing is necessary to enable the physician to offer the most suitable therapy for a patient with advanced NSCLC.

Four *EGFR* mutation tests, PCR-Invader® [4], peptide nucleic acid-locked nucleic acid (PNA-LNA) PCR clamp [5], PCR direct sequencing [6], and Cycleave PCR™ [7] are used commercially in Japan, with testing generally carried out by centralized contracted laboratories. The Scorpion Amplification Refractory Mutation System (ARMS)® [8] is another sensitive globally available method and in particular was used in the phase III Iressa Pan-Asia Study (IPASS) to determine *EGFR* mutation status [1, 9]. A variety of methods, including direct sequencing, PCR-Invader, PNA-LNA PCR clamp, fragment analysis, and Cycleave PCR, were used in the WJTOG3405 phase III study to select *EGFR* mutation-positive patients [2], and the PNA-LNA PCR clamp method was used in the NEJ002 study [3]. To date, a study to compare the sensitivity and concordance of methods for *EGFR* mutation testing in Japan has not been conducted.

Diagnostic practices, and therefore, samples available for *EGFR* mutation analysis, differ between laboratories and countries. Large surgical samples are optimal for *EGFR* mutation analysis but small tissue from a tumor biopsy is the most commonly used and preferred sample type for diagnosis by clinicians [10, 11]. In clinical practice, tissue samples are not always available for diagnosis, and cytology samples, including bronchofiberscopic brushing (BB) cytology and pleural effusion cytology samples, are used in Japan and increasingly globally.

The aim of this study was to evaluate the sensitivity and performance of different *EGFR* mutation tests using artificial DNA admixtures, and clinical samples including formalin-fixed

*Correspondence to: Dr K. Goto, Division of Thoracic Oncology, National Cancer Center Hospital East, Kashiwanoha, 6-5-1, Kashiwa, Chiba, 277-8577, Japan. Tel: +81-4-7133-1111; Fax: +81-1-7131-4724; E-mail: kgoto@east.ncc.go.jp